Insights into the autotransport process of a trimeric autotransporter, Yersinia Adhesin A (YadA).

Nandini Chauhan[1,2,*], **Daniel Hatlem**[1,*], **Marcella Orwick-Rydmark**[1], **Kenneth Schneider**[1], **Matthias Floetenmeyer**[2,3], **Barth van Rossum**[4], **Jack C. Leo**[1,2], **Dirk Linke** [1,2,*]

[1] Department of Biosciences, University of Oslo, Blindernveien 31, 0371, Oslo (Norway)

[2] Max-Planck-Institute for Developmental Biology, Department 1, Tübingen (Germany)

[3] The Centre for Microscopy and Microanalysis, the University of Queensland, 4072, St. Lucia Queensland (Australia)

[4] Forschungsinstitut für Molekulare Pharmakologie, Department of NMR-Supported Structural Biology, Berlin, Germany

- These authors contributed equally

Abstract

Trimeric autotransporter adhesins (TAAs) are a subset of a larger protein family called the type V secretion systems. They are localized on the cell surface of Gram-negative bacteria, function as mediators of attachment to inorganic surfaces and host cells, and thus include important virulence factors. *Yersinia* adhesin A (YadA) from *Yersinia enterocolitica* is a prototypical TAA that is used extensively to study the structure and function of the type V secretion system. A solid-state NMR study of the membrane anchor domain of YadA previously revealed a flexible stretch of small residues, termed the ASSA region, that links the membrane anchor to the stalk domain. In this study, we present evidence that single amino acid proline substitutions produce two different conformers of the membrane anchor domain of YadA; one with the N-termini facing the extracellular surface, and a second with the N-termini located in the periplasm. We propose that TAAs adopt a hairpin intermediate during secretion, as has been shown before for other subtypes of the type V secretion systems. As the YadA transition state intermediate can be isolated from the outer membrane, future structural studies should be possible to further unravel details of the autotransport process.

Introduction

The cell envelope of Gram-negative bacteria comprises three layers: a cytoplasmic membrane, a peptidoglycan layer in the periplasm, and an asymmetric outer membrane (OM) consisting of an inner leaflet of phospholipids and an outer leaflet made of lipopolysaccharide (LPS). To export

proteins to the cell surface, Gram-negative bacteria have evolved a number of specialized secretion systems that allow protein substrates to traverse both membranes and the periplasmic space. Type V secretion systems are one of these; they are popularly known as autotransporters (ATs) as they do not require external energy sources for their export mechanism (Thanassi *et al.*, 2005). Their domain architecture includes a β-barrel transmembrane domain that anchors the protein in the outer membrane and that hosts the secretion function, and an extracellular region or passenger that typically comprises repeats that make up a fibrous structure (Leo *et al.*, 2012, Hartmann *et al.*, 2012, Szczesny & Lupas, 2008).

Type V secretion is a two-step process. First, the Sec machinery facilitates transport through the cytoplasmic membrane (Natale *et al.*, 2008), and then the actual 'autotransport' occurs in the outer membrane (Fan *et al.*, 2016, Leo *et al.*, 2012). For this process, various external factors are necessary, which include periplasmic chaperones to keep the polypeptide chain in an export-competent state (Ruiz-Perez *et al.*, 2010, Ruiz-Perez *et al.*, 2009), and the BAM (β-barrel assembly machinery) complex that inserts the transmembrane pore domain of the type V secretion system into the outer membrane (Plummer & Fleming, 2016, Bakelar *et al.*, 2016, Sauri *et al.*, 2009, Ieva & Bernstein, 2009, Lehr *et al.*, 2010).

The mechanism of autotransport is poorly understood, and one of the open questions is the role of the BAM complex and possibly of the partly paralogous TAM (translocation and assembly) machinery in the secretion of the passenger (Jeeves & Knowles, 2015); TAM involvement has been excluded for at least two TAA examples (Saragliadis *et al.*, 2018). Additional complexity is added by type V secretion systems being subdivided into the classes type Va through type Ve based on structural differences (Leo *et al.*, 2012). Figure 1 summarizes the models of autotransport for the type Va (Classical) (Junker *et al.*, 2009) and type Ve (Inverse) ATs (Oberhettinger *et al.*, 2015) that have both been shown to translocate their passenger domains via a hairpin intermediate. Formation of a hairpin initiates the transport process that proceeds from the C- to N-terminus in type Va systems, and from the N- to C-terminus in type Ve systems. While the entry of the passenger into the lumen of the β-barrel domain is an energetically unfavorable process, the coupling to the (energetically favored) folding and outer membrane insertion of the β-barrel itself would make this transition state more feasible (Drobnak *et al.*, 2015). The passenger domain must remain unfolded during the complete process, as higher order structures would block the

translocation (Leyton *et al.*, 2011, Adams *et al.*, 2005). For both the type Va and the type Ve systems, it has been shown that the part of the passenger proximal to the barrel emerges first (Junker *et al.*, 2009, Oberhettinger *et al.*, 2015), and it has been speculated that the passenger domain folds as it emerges from the barrel, which would serve as the source of free energy to pull out rest of the passenger domain from the barrel pore sequentially (Drobnak *et al.*, 2015, Oberhettinger *et al.*, 2015, Leo *et al.*, 2016). The BAM complex seems to be involved not only in β-barrel assembly, but also in passenger translocation, as stalled passenger translocation intermediates for both Type Va and Ve secretion systems were found associated with BamA (Oberhettinger *et al.*, 2015, Roman-Hernandez *et al.*, 2014, Ieva & Bernstein, 2009), although the mechanism for this process is still unclear.

In this work, we set out to investigate whether type Vc autotransporters, also called Trimeric Autotransporter Adhesins (TAAs) (Linke *et al.*, 2006), initiate transport via a hairpin intermediate in a mechanism comparable to other autotransporters, using the prototypical *Yersinia* adhesin A (YadA) as our established model system (Muhlenkamp *et al.*, 2015, Leo *et al.*, 2012). YadA from the human pathogens *Yersinia enterocolitica* and *Y. pseudotuberculosis* is an obligate homotrimeric protein with a 12-stranded transmembrane β-barrel domain, where each protomer contributes four strands to the final structure (Shahid *et al.*, 2012a). The passenger of YadA consists of a trimeric coiled-coil stalk domain (Alvarez *et al.*, 2010) and a sticky globular head domain (Nummelin *et al.*, 2004). The stalk and the β-barrel are connected by a linker region (Figure 2A) that is essential for passenger translocation and for trimerization of the β-barrel of TAAs (Roggenkamp *et al.*, 2003, Meng *et al.*, 2006). The linker along with the β-barrel is sufficient for membrane insertion (Wollmann *et al.*, 2006, Mikula *et al.*, 2012), indicating that the linker of TAAs plays an important role in their biogenesis. Molecular dynamics simulations of the translocator domain of the TAA Hia from *Haemophilus influenzae* has shown that the linker forms stabilizing interactions with the β-sheet of the barrel, which in turn stabilize the trimeric barrel (Holdbrook *et al.*, 2013).

The linker region (marked in Figure 2) comprises a stretch of residues with unusual properties. In an earlier solid-state NMR study on YadA, we showed that the so-called ‘ASSA’ region, relevant for this potential hairpin, consists exclusively of small residues and is highly flexible even in the final, folded state – both important prerequisites for a potential hairpin in a confined space. (Shahid

et al., 2012a, Shahid *et al.*, 2012b). Sequence alignments of YadA with other TAAs showed no direct sequence conservation of the ASSA motif, but that the residues occupying the linker region are always small in size and of lower predicted helical propensity (Shahid *et al.*, 2012a). In order to study the importance of this part of the linker, we introduced single proline substitutions in the 'ASSA' region to deliberately reduce its flexibility. If 'ASSA' forms the hairpin core, then introducing a proline, an established secondary structure breaker that does not allow for rotation of the peptide backbone without breaking a covalent bond, should stall the translocation process – and could potentially capture a hairpin in a locked conformation. Using assays to study the oligomeric state, membrane insertion of the β-barrel domain, and surface exposure of the passenger domain, we then tested how the mutation affected autotransport. In the course of this work, we found that the SpyCatcher system (Zhang *et al.*, 2013) is a very powerful tool to assay surface exposure of translocated proteins in bacteria, and modified the system by fusing it to GFP for easier visualization, e.g. during semi-native SDS-PAGE.

Materials and Methods

DNA constructs and mutagenesis.

The pASK-IBA2-based constructs of full-length YadA and membrane anchor YadAM were used from earlier work (Grosskinsky *et al.*, 2007, Wollmann *et al.*, 2006). Site directed mutagenesis was used to introduce single amino acid mutations (Byrappa *et al.*, 1995). The mutagenesis PCR was carried out using a pair of phosphorylated primers containing the desired mutation and Phusion DNA polymerase (New England Biolabs). Methylated parental DNA was removed by treating the PCR product with 10 units of DpnI (New England Biolabs) for one hour at 37 °C. The blunt end PCR products were subsequently ligated using 2000 units of T4 ligase (New England Biolabs) for one hour at room temperature. The ligation mix was then directly transformed into chemically competent *E. coli* Top10 cells (Invitrogen) and mutants were confirmed by DNA sequencing. Mutants created for this study include: $YadAM_{G352P}$, $YadAM_{L353P}$, $YadAM_{A354P}$, $YadAM_{S355P}$, $YadAM_{S356P}$, $YadAM_{A357P}$, $YadAM_{A358P}$, and $YadAM_{L359P}$ and $YadA_{A354P}$, where the latter is a full-length YadA construct. Primers are listed in Table 1.

A sequence encoding a Spytag (AHIVMVDAYKPTK) (Zakeri *et al.*, 2012) was introduced between the signal peptide and the beginning of the $YadA_{wt}$/$YadA_{A354P}$ sequence by Gibson assembly (Gibson *et al.*, 2009) to yield the constructs Spy-$YadA_{wt}$ and Spy-$YadA_{A354P}$. The Spytag sequence was produced as overlapping oligonucleotides with ends complementary to the OmpA signal peptide of the pASK-IBA2 vector at the 5' end and the YadA sequence at the 3' end. $YadA_{wt}$ and $YadA_{A354P}$ were then amplified by PCR so that the 3' end of the product was complementary to the pASK-IBA2 vector. These were then assembled using the Gibson reaction and transformed into the *E. coli* Top10 strain. Positive clones were screened for by colony PCR, and verified by DNA sequencing. DNA encoding maltose-binding protein (MBP or MalE) was amplified from pMal-c2 (New England Biolabs). This was fused to SpyTag similarly to YadA and cloned into pASK-IBA2. The resulting plasmid (pIBA2-SpyTag-MBP) includes an OmpA signal peptide for periplasmic targeting. The Spy-tagged membrane anchor constructs Spy-$YadAM_{wt}$ and Spy-$YadAM_{A354P}$ were created similarly, and in addition included a Strep II tag (called Strep tag hereafter) for detection in Western blots. The primers were designed such that only the Spytag and the membrane anchor part of $YadA_{wt}$ and $YadA_{A354P}$ were amplified by PCR.

For creating fusion constructs of SpyCatcher with superfolded green fluorescent protein (sfGFP), the sfGFP coding sequence was amplified with its 5' end complimentary to the respective SpyCatcher sequence and 3' end complimentary to the vector, pASK-IBA3. The template was pCX-sfgfp, kindly provided by Friedrich Götz (University of Tübingen) (Yu & Gotz, 2012). $SpyCatcher_{wt}$ and $SpyCatcher_{EQ}$ were amplified with their 5' end complimentary to pASK-IBA3. The template plasmids pDEST14-SpyCatcher (Addgene plasmid #35044) and the control plasmid pDEST14-SpyCatcher EQ (Addgene plasmid #35045) were a gift from Mark Howarth (University of Oxford). The sfGFP PCR product was then fused with $SpyCatcher_{wt}$ and $SpyCatcher_{EQ}$ using PCR and cloned into the pASK-IBA3 vector using Gibson assembly, yielding $SpyCatcher_{wt}$-sfGFP and $SpyCatcher_{EQ}$- sfGFP.

Table 1 Primers used for cloning of new constructs

	Primers used
G352P	**Fwd: GTT GAC AAA CCT TTA GCC AGT** **Rev: TCG TGT GTC AAG TTT ATC TAA ACG GTT GTC**
L353P	**Fwd: GTT GAC AAA GGT CCA GCC AGT**

	Rev: TCG TGT GTC AAG TTT ATC TAA ACG GTT GTC
A354P	**Fwd**: **CCG AGT TCA GCC GCT TTA AAC AGC TT** **Rev: TAA ACC TTT GTC AAC TCG TGT GTC**
S355P	**Fwd: GTT GAC AAA GGT TTA GCC CCA TCA GCC GCT** **Rev: TCG TGT GTC AAG TTT ATC TAA ACG GTT GTC**
S356P	**Fwd: GTT GAC AAA GGT TTA GCC AGT CCA GCC GCT** **Rev: TCG TGT GTC AAG TTT ATC TAA ACG GTT GTC**
A357P	**Fwd: TTA GCC AGT TCA CCC GCT TTA AAC AGC TTG TTC CAG** **Rev: ACC TTT ATC AAC TCG TGT GTC AAG**
A358P	**Fwd: TTA GCC AGT TCA GCC CCT TTA AAC AGC TTG TTC CAG** **Rev: ACC TTT ATC AAC TCG TGT GTC AAG**
L359P	**Fwd: TTA GCC AGT TCA GCC GCT CCA AAC AGC** **Rev: ACC TTT ATC AAC TCG TGT GTC AAG**
SpyCatcher	**Fwd: TAA CGA GGG CAA AAA ATG CAC CAT CAC CAT CAC CAT GGC GCC ATG GTT GAT ACC TT** **Rev: AAT ATG AGC GTC ACC TTT AGT TG**
Spycatcher-sfGFP	**Fwd: AAA GGT GAC GCT CAT ATT GGC GGT TCA AAA GGT GAA GAA TTA TTT A** **Rev: CGG GTG GCT CCA AGC GCT TTT ATA TAA TTC ATC CAT ACC ATG TG**
pAsk-IBA3	**Fwd: GCG CTT GGA GCC ACC CG** **Rev: CAT TTT TTG CCC TCG TTA TCT AGA T**
Spytag-(YadAM/YadAM-A354P)	**Fwd: CAT AAA TTC CAT CAA CTT GAC** **Rev**: **TTT GGT CGG TTT ATA TGC ATC**
SpyTag forward	**Fwd: ACC GTA GCG CAG GCC GCC CAT ATT GTT ATG GTG GAT GCA TAT AAA C**
SpyTag-YadA	**Fwd: AAC CTC GTC ATT ATT TTT GGT CGG TTT ATA TGC ATC CAC CAT A**
SpyTag-MBP	**Fwd: ACC TTC TTC GAT TTT GCT AGA TTT GGT CGG TTT ATA TGC ATC CAC CAT A**
YadA	**Fwd: AAT AAT GAC GAG GTT CAT TTT ACA G** **Rev: GTG GCT CCA AGC GCT CTA TTA CCA CTC GAT ATT AAA TGA TGC AT**
MBP	**Fwd: AAA ATC GAA GAA GGT AAA CTG GTA ATC T** **Rev: GTG GCT CCA AGC GCT AGT CTG CGC GTC TTT CAG G**

Strains and Growth conditions

The *E.coli* BL21ΔABCF strain (*E.coli* BL21(DE3) Δ(*ompA, lamB, ompC, ompF*)) was used for overexpression of most constructs (Meuskens *et al.*, 2017). For SpyCatcher assays, *E. coli* BL21-Gold(DE3) was used (Merck). Cells were grown in low-salt Lysogeny Broth (LB) (Tryptone-10 g, Yeast extract-5 g and NaCl-5 g) with 100 μg/mL of ampicillin at 30 °C. An overnight culture was used to inoculate fresh LB medium. For protein production and purification, bacteria were grown to OD_{600} of 0.6 and induced with 0.05 – 0.1 μg/mL of AHTC overnight.

Protein production and purification

$YadAM_{wt}$ and $YadAM_{A354P}$ were produced and purified for the heat stability assays, FTIR spectroscopy, and other studies as previously described (Wollmann *et al.*, 2006), with some changes. In brief, the cell pellets suspended in lysis buffer (Phosphate-Buffered Saline (PBS) with 1mM $MgCl_2$ and a pinch of DNase I) were lysed using a French pressure cell (Thermo). The lysates were subjected to ultracentrifugation in a Beckman Ti45 rotor at 70000 × *g* for 1 hour. The pellet was resuspended in inner membrane solubilization buffer (20 mM Tris at pH 8 and 1% N-lauroylsarcosine) for 1 hour at room temperature on a rocking shaker followed by ultracentrifugation as above. The resulting outer membrane pellet was washed with water and was then resuspended in outer membrane solubilization buffer (20 mM Tris/HCl pH 8.0, 150 mM NaCl, 10 mM dithiothreitol, 50 mM EDTA, 0.1 mg/mL lysozyme and 3% (w/v) octyl-polyoxyethylene (C_8POE, (Bachem)) for 2 h at room temperature followed by ultracentrifugation to remove debris. The sample was then directly purified using cation exchange chromatography after a 1:3 dilution with water to reduce the ionic strength of the buffer. A phase separation step (Wollmann *et al.*, 2006) was avoided because the mutant protein was not stable enough to withstand it. Cation exchange chromatography was performed using a Mono S 5/50 GL (GE healthcare) column on a BioRad NGC System. 25 mM MES (pH 6), 50 mM NaCl and 1% C_8POE was used for column equilibration and the protein was eluted using a gradient of 50 mM to 1 M NaCl. 25 mM MES buffer at pH 6 was used instead of 25 mM MOPS (pH 7) as $YadAM_{A354P}$ was more stable in this buffer condition.

$Spycatcher_{wt}$-sfGFP was produced in *E.coli* BL21(DE3) Gold (Novagen) and induced with 0.1 µg/mL AHTC followed by 4 hours of expression. The cells were harvested by centrifugation at 3100 × *g* for 15 min. The pellets were resuspended in Ni-NTA equilibration buffer (20 mM phosphate buffer at pH 7.4, 200 mM NaCl and 20 mM imidazole) containing 1 mM MgCl2, a pinch of DNase I and EDTA-free protease inhibitor cocktail (Pierce). The cell suspensions were lysed using a French pressure cell and the lysate was centrifuged at 70000 × *g* for 30 min. The supernatants were applied to a 5 mL His Trap HP Ni-NTA column (GE Healthcare) equilibrated with Ni-NTA equilibration buffer and eluted with a 20 mM to 500 mM imidazole gradient using a Bio-Rad NGC chromatography system. The fractions containing the SpyCatcher proteins were pooled and dialyzed against PBS overnight at 4 °C.

Trimer stability assay and urea extraction:

To assess trimer stability, purified $YadAM_{wt}$ and $YadAM_{A354P}$ were treated with 4 M urea in SDS-PAGE sample buffer (100 mM Tris-HCl pH 6.8, 8% SDS, 40% glycerol, 2 mM EDTA, 0.1% bromophenol blue) and heated to 85 °C for different times. The samples were then separated on 15% SDS-polyacrylamide gels (SDS-PAGE) and visualized by silver staining (Nesterenko *et al.*, 1994).

Membrane insertion of $YadAM_{wt}$ and $YadAM_{A354P}$ was assessed by urea extraction as previously described (Leo *et al.*, 2015b). In brief, cells from 100 mL culture volume were lysed using a French pressure cell followed by inner membrane solubilization as described above. The outer membrane pellet obtained after ultracentrifugation was resolubilized in 1 mL urea extraction buffer (15 mM Tris at pH 7.4, 100 mM glycine and 6 M urea) and incubated for one hour at 37 °C. The membrane pellet was collected by ultracentrifugation at 290000 × *g* for 90 min at 25 °C. The supernatant was removed and the pellet was resuspended in 1 mL ultrapure water. The samples were analyzed in a 15% SDS-PAGE gel by staining it with colloidal Coomasie-G250.

Fourier transform infrared (FTIR) spectroscopy

FTIR spectra of purified $YadAM_{wt}$ and $YadAM_{A354P}$ were acquired on Bruker Optics Tensor27 as described (Wollmann *et al.*, 2006). Purified $YadAM_{wt}$ and $YadAM_{A354P}$ protein samples were dialyzed overnight at 4 °C in a buffer solution containing 25 mM MES at pH 6, 50 mM NaCl and 1% C_8POE. The buffer from dialysis was used as a blank for background measurements. The spectra were measured at 25 °C through accumulation of 120 FTIR scans at a resolution of 4 cm^{-1}. The proprietary data analysis software OPUS provided by Bruker Optics was used to calculate the α-helical and β-sheet content, and protein concentration in each sample. The software makes use of a database containing the FTIR spectra of proteins with known secondary structure to calculate the secondary structure content of sample proteins.

Electron microscopy

E. coli cells expressing $YadA_{wt}$ and $YadA_{A354P}$ were treated with 2% formaldehyde in 0.1 M cacodylate buffer pH 7.4 for 30 min followed by washing with 200 mM glycine in PBS and 0.2% Bovine Serum Albumin (BSA) in PBS for 10 min. YadA was labelled with rabbit polyclonal anti-YadA antiserum (Grosskinsky *et al.*, 2007) in 0.2% BSA in PBS for one hour followed by washing three times with 0.2% BSA in PBS. The primary antibody was labelled with Protein A-conjugated

10 nm gold particles in 0.2% BSA in PBS for an hour. The cells were washed three times with 0.2% BSA in PBS and 3 times with PBS followed by fixing with 2.5 % glutaraldehyde for an hour. Samples were embedded in 2% gelatin and then cut into blocks that were incubated with OsO_4 on ice for an hour. The blocks were washed twice with water and incubated with uranyl acetate at 4 °C. The blocks were then embedded in Epon and thin sectioned by following standard protocols (Grin *et al.*, 2011).

Autoaggregation Assay

Bacterial cultures were grown as described above. After 2 h of induction under shaking at 200 rpm, the cells were pelleted by centrifugation at 3100 x g for 10 min and resuspended in PBS. Autoaggregation was measured by a sedimentation assay: The initial OD_{600} was measured and the culture was kept undisturbed at room temperature. Aliquots from the surface of the culture were taken every 20 min over a two-hour incubation period and the OD_{600} was measured. A picture of the bacterial culture was taken at the end of the experiment (after 2 h of static incubation).

Outer membrane preparation

Small-scale outer membrane isolation was performed using differential detergent solubilization, as previously described (Leo *et al.*, 2015b). An amount of cells corresponding to 40 mL at OD_{600} = 1.0 was pelleted by centrifugation, and resuspended in 1.5 mL 10 mM HEPES pH 7.4, 10 mM $MgCl_2$, 0.1 mg/mL lysozyme, and a pinch of DNase I. Cell suspensions were transferred to 2 mL screw-cap tubes containing glass beads (BioSpec Products, 0.1 mm diameter) and were lysed using the default bacterial lysis protocol (2 x 3 minutes of shaking, with 3 minutes cooling down between) on a SpeedMill Plus (Analytik Jena). Samples were centrifuged for 2 min at 15600 × *g* to remove cell debris (This step had to be omitted from outer membrane preparations of full-length constructs due to YadA-mediated autoaggregation of the vesicles – the resulting preparations were enriched for outer membranes but less pure). The lysate was then transferred to a 1.5 mL microcentrifuge tube and centrifuged at 15600 × *g* for 30 min. The pellet was resuspended in 0.2 mL 10 mM HEPES, pH 7.4 and an equal volume of 2% N-lauroylsarcosine was added for selective solubilization of the inner membrane (Orwick-Rydmark *et al.*, 2016). Samples were incubated on a shaker at room temperature for 30 min. The suspension was then centrifuged for 30 min at 15600 × *g* to pellet the outer membrane and the pellet was washed once with 0.5 mL of 10 mM HEPES,

pH 7.4 followed by centrifugation at 15600 x g for 10 min. The pellet was then suspended in 60 µL 10 mM HEPES, pH 7.4 and 20 µl 4X SDS-PAGE sample buffer. The samples were directly used for SDS-PAGE analysis, or stored at -20^{o}C.

Spytag-SpyCatcher assays

Fluorescence quantification using a plate reader: For this particular assay, a 10 mL culture volume was used and bacteria were induced with 0.005 µg/mL of AHTC for 2 hours. *E. coli* BL21-Gold(DE3) cells expressing Spytagged $YadA_{wt}$, $YadA_{A354P}$, $YadAM_{wt}$ and $YadAM_{A354P}$ (each having three biological replicates) corresponding to OD_{600} = 1 were collected by centrifugation at 3100 x g. The cells were resuspended in 1 mL PBS. To 500 µl of cells, 20 µl $SpyCatcher_{wt}$-sfGFP (10 mg/mL) was added and to the other 500 µl, 20 µl of the control protein $SpyCatcher_{EQ}$-sfGFP (10 mg/mL) was added followed by incubation at RT for an hour. The cells were washed three times with PBS and finally resuspended in 200 µl PBS. The fluorescence (absorbance-488 nm, emission-533 nm) was measured using a black 96 well polystyrene plate on a plate reader (Biotek-Synergy H1).

***SDS-PAGE gel analysis of SpyCatcher assays*:** BL21(DE3) cells expressing $YadAM_{wt}$, $YadAM_{A354P}$, and pASK-IBA2 were induced with 0.1 µg/mL AHTC and incubated for 3 hours. An amount of cells corresponding to 80 mL culture at OD_{600} = 1 was pelleted by centrifugation at 3000 × *g* for 5 minutes, washed once, and and resuspended in 3 mL PBS. The samples were split into two aliquots. To one aliquot, 90 µl of 20 mg/mL $SpyCatcher_{wt}$-sfGFP was added and incubated for 1 hour. The samples were then washed three times with 1.5 mL 10 mM HEPES, pH 7.4 prior to outer membrane preparation as described above. The other aliquots were washed once with 1.5 mL 10 mM HEPES, pH 7.4, and lysed as described for the outer membrane preparation protocol. 150 µL 10X PBS and 90 µl 20 mg/mL $SpyCatcher_{wt}$-sfGFP were added to the lysate and incubated for one hour prior to OM preparation of the sample as described above (omitting the lysis step). The full-length $YadA_{wt}$ and $YadA_{A354P}$-expressing cells were treated with both $SpyCatcher_{wt}$-sfGFP and $SpyCatcher_{EQ}$-sfGFP (as control) under the same conditions as mentioned above, omitting the 2 minute centrifugation step due to autoaggregation of the OM-vesicles after lysis in the wildtype YadA sample. The outer membrane preparations of each of these samples were analysed on 12% SDS-PAGE and Bolt 4-12% Bis-Tris Plus Gels. The protein bands for $SpyCatcher_{wt}$-sfGFP-treated

samples were visualized under blue light to view the fluorescent bands and then stained with Coomassie R-250 as necessary.

***SpyCatcher assay with periplasmic MBP*:** BL21-Gold(DE3) cells were transformed with either pIBA2-SpyTag-MBP or pASK-IBA2 (vector control). An overnight culture grown in LB with 100 mg/mL ampicillin was diluted 1:50 in fresh medium and grown at 37 °C to mid-log (OD_{600} ~0.5). The incubation temperature was then changed to 30 °C for 30 minutes before induction with AHTC (0.05 µg/mL). The cultures were incubated for 2 hours before the OD_{600} was measured and an amount of cells corresponding to 40 mL at OD_{600} = 1.0 was pelleted for 15 minutes at 4000 × *g*. This was performed in duplicate. The samples were resuspended in PBS and $SpyCatcher_{wt}$sfGFP or $SpyCatcher_{Eq}$-sfGFP was added to the samples to a final concentration of 10 µM in a total volume of 2 mL. Then the sample was split into two 1-mL aliquots that were incubated at room temperature for 1 hour with gentle rotation. At the end of the incubation, one duplicate was washed 3 times with PBS, whereas the other was not. The samples were then transferred to 2 mL screw cap tubes, to which ~0.25 mL of 0.1 mm glass beads had been added. The cells were subjected to lysis using a bead beater (BioTechne FastPrep FP120), 2 x 40 seconds at speed setting 5.0, with 5 minutes cooling on ice in between. After lysis, the lysates were cooled on ice for 5 minutes and then incubated for 30 minutes at room temperature with rotation. They were then centrifuged for 5 minutes at 16000 × *g*. For analysis, a sample of the resulting supernatant was taken and mixed at a ratio of 3:1 with 4 x SDS-PAGE sample buffer. The samples were separated in a 4-20% gradient gel (Novex Tris-Glycine, ThermoFisher) and transferred to a Protran nitrocellulose mebrane (GE Healthcare) using a semi-dry apparatus (Hoefer). After transfer, the membranes were blocked with PBS containing 2% w/v skimmed milk powder for 1 hour at room temperature with shaking (60 rpm). An anti-MalE antibody (Leo *et al.*, 2015a) was added diluted 1:10000 in blocking buffer. After an hour's incubation as above, the membrane was washed twice with PBS-T (PBS with 0.05% Tween20), after which an anti-rabbit antibody-CF®770 conjugate (Biotium) was added diluted 1:10000 in blocking buffer. The membrane was incubated for an hour as above and then washed three times with PBS-T. The secondary antibody was detected using a LI-COR Odyssey CLx system.

Spycatcher assays in the periplasm: To detect passenger domain N-termini located in the periplasm due to potential stalling of the autotransport process, *E.coli* BL21 were transformed with

pIBA2 vectors containing the constructs Spy-YadA$_{wt}$/Spy-YadA$_{A354P}$ or Spy-YadAM$_{wt}$/Spy-YadAM$_{A354P}$. The transformants were then co-transformed with a vector for the expression of periplasmic SpyCatcher$_{wt}$ and SpyCatcher$_{EQ}$ in pACYC-duet. The resulting combinations of double-transformants are shown in Table 2.

Table 2: Nomenclature of SpyCatcher$_{wt}$ and SpyCatcher$_{EQ}$ transformant combinations

***E.coli* BL21 Gold (DE3)**	**Spy- and StrepTagged full length YadA wild type**	**Spy- and StrepTagged full length YadA proline mutant**	**Spy- and StrepTagged membrane anchor YadA wild type**	**Spy- and StrepTagged membrane anchor YadA proline mutant**	**Non-modified pIBA2 control plasmid**
Periplasmic SpyCatcher$_{wt}$	SpyC$_{wt}$-YadA$_{wt}$	SpyC$_{wt}$-YadA$_{A354P}$	SpyC$_{wt}$-YadAM$_{wt}$	SpyC$_{wt}$-YadAM$_{A354P}$	SpyC$_{wt}$-pIBA2
Periplasmic SpyCatcher$_{EQ}$	SpyC$_{EQ}$-YadA$_{wt}$	SpyC$_{EQ}$-YadA$_{A354P}$	SpyC$_{EQ}$-YadAM$_{wt}$	SpyC$_{EQ}$-YadAM$_{A354P}$	SpyC$_{EQ}$-pIBA2
None modified pACYC control plasmid	pACYC-YadA$_{wt}$	pACYC-YadA$_{A354P}$	pACYC-YadAM$_{wt}$	pACYC-YadAM$_{A354P}$	pACYC-pIBA2

For the detection of Spy-tagged protein in the periplasm, YadA/YadAM expression was induced in double-transformants at the mid-exponential growth phase (with 0.1 μg/mL AHTC) for one hour before periplasmic SpyCatcher was induced (0.5mM IPTG) during the following hour. The incubation temperature was lowered from 37°C to 30°C as soon as the AHTC was added. Premature induction of SpyCatcher expression was prevented through elevated levels of glucose (0.5% w/v) in the ZYP induction medium during the YadA/YadAM expression. In between the two induction steps, cells were pelleted and washed in glucose-free ZYP medium. To check for

leakiness of the outer membrane for periplasmic SpyCatcher, aliquots of the supernatants after each induction step were collected and subjected to Western blotting. The risk of labelling the extracellular Spy-YadA/YadAM through the release of periplasmic SpyCatcher during cell lysis was minimized by adding an excess (10μM) of SpyTag fusion peptide (CASLO, lot.no.: P220617-01-01) to the samples before lysis in 8 mol/L urea at 95°C for 15 minutes. The released DNA was sheared through 27G syringe needles before samples were assessed on SDS-PAGE gels as described above.

Mass spectrometry analysis

A band excised from a gradient SDS-PAGE (See supplementary Figure S1) was suspended in 10% acetic acid, and was analyzed at the mass spectrometry core facility at the Department of Biosciences, University of Oslo. Briefly, bands were in-gel digested with trypsin followed by extraction of the peptides from the gel. These were applied to a Dionex Ultimate 3000 RSLCnano-UHPLC system (Sunnyvale, CA, USA) coupled online to an LTQ-Orbitrap XL mass spectrometer (Thermo Electron, Bremen, Germany) equipped with a nanoelectrospray ion source. Data were acquired using Xcalibur v2.5.5 and raw files were processed to generate peak list in Mascot generic format (*.mgf) using ProteoWizard release version 3.0.331. Database searches were performed using Mascot in-house version 2.4.0 to search the SwissProt database (Bacteria, 332,372 sequences). For full methodology, see Supplementary Material.

Quantification of YadAM$_{wt}$ and YadAM$_{A354P}$ protein expression in the outer membrane by SDS-Page analysis: Fresh transformants of BL21ΔABCF containing YadAM$_{wt}$, YadAM$_{A354P}$ or an empty vector control were grown overnight and used to inoculate (1:50) 300 mL of media. Cultures were induced at OD_{600} = 0.5, and grown overnight. The OD_{600} after overnight incubation was measured, volumes with equal numbers of cells were collected for each construct, and all samples were centrifuged at 3000 x *g*. Cells were resuspended in buffer (50 mM Tris pH 7.4, 50mM NaCl, 1 mM each $MgCl_2$ and $MnCl_2$, 200 μg/mL lysozyme, 20 ug/mL DNAse I), and incubated on ice for approximately 15 minutes before passage through a French pressure cell (three passes). For extraction of the OMs, cells were pelleted at 3000 × *g* for 20 minutes to remove unbroken cells, resuspended in fresh buffer, and pelleted at 100000 × *g* for 1 hour to collect the membrane fraction. Inner membranes were solubilized for 1 hour in 30 mL buffer containing 1% N-laurylsarcosyline,

20 mM HEPES pH 8.0, and spun again at 100000 × *g* for 1 h to collect the OM fraction. The OM fraction was resuspended twice in 20 mM HEPES pH 8.0 and centrifuged to remove residual detergent.

To fully extract and monomerize $YadAM_{wt}$ and $YadAM_{A354P}$ from the OM, samples were resuspended in 1 mL buffer containing 8 M Urea, 1 mM EDTA, 20 mM Tris pH 7.4, and passed through a 27G needle in order to shear the DNA. 125 µl of each sample were mixed with an equal volume of buffer, and incubated overnight at 95 °C. The samples were taken from the heat block, allowed to cool, and 4X SDS-PAGE sample buffer was added to 1X, and the samples were allowed to incubate for 1 hour at 50 °C. The samples were further diluted 1:2 in 4X SDS-PAGE sample buffer, and 10 µl of each sample was loaded onto 6 M Urea SDS-PAGE gels (Schagger, 2006) and run at 40 mA for 90 minutes. Gels were stained using Coomassie Blue R-250, followed by visualization and quantification using a Kodak Image Station 4000R with Carestream software (Molecular Imaging Software).

Results

Effect of proline substitutions in the 'ASSA' region.

In order to study the role of the 'ASSA' region in the autotransport of YadA, single amino-acid mutants carrying a proline substitution were created. The initial analysis was done using the YadA membrane anchor constructs (YadAM) lacking most of the passenger, as these are easier to purify due to the smaller size (Wollmann *et al.*, 2006) and due to the lack of the head domain that is responsible for adhesion and autoaggregation (Muhlenkamp *et al.*, 2015).

$YadAM_{wt}$ migrates as a trimeric protein with an apparent molecular weight of 45 kDa while the denatured YadAM monomer has a molecular weight of 12 kDa when subjected to SDS-PAGE (Wollmann *et al.*, 2006). All four proline mutants in the 'ASSA' region ($YadAM_{A354P}$, $YadAM_{S355P}$, $YadAM_{S356P}$, $YadAM_{A357P}$) remain folded in unheated samples and have a similar apparent molecular weight on semi-native SDS-PAGE gels that is higher than the expected monomer band, but lower than that of the wild-type protein (Figure 3). In order to check if this effect extends to the residues beyond the 'ASSA' region, single amino acid proline substitutions were introduced into flanking residues on either side of the 'ASSA' region. $YadAM_{L353P}$ and $YadAM_{A358P}$ do not show the same migration behavior as the proline mutants of the 'ASSA' region,

but still migrate faster than $YadAM_{wt}$ (Figure 3). Note that the gel system is "semi-native", i.e. that the samples were not heated before electrophoresis, and that trimers of YadA or YadAM constructs remain intact under these conditions when not heated in urea buffers excessively (Wollmann *et al.*, 2006, Grosskinsky *et al.*, 2007). A possible explanation for the differences in migration behavior of all the proline mutants compared to $YadAM_{wt}$ is that different amounts of SDS molecules bound to each mutant trimer, which would point to significant changes in tertiary and quaternary structure. A previous study on anomalous migratory behavior of point mutants of membrane proteins in SDS-PAGE indicates that conformational changes caused by point mutations can indeed lead to altered SDS binding (Rath *et al.*, 2009). This in turn increases or decreases the overall negative charge on the protein and thereby affects the migration in SDS-PAGE. We saw no indication of systematic proteolytic degradation of any of the fragments – see also trimer labeling results further below. All expressed mutants could be detected with an anti-StrepTag antibody targeting the N-terminal tag, and thus are not truncated by proteases (data not shown). The mutant L359P was not expressed in the membrane at all under various tested conditions, and the mutant A358P showed lower expression levels than the ASSA mutants. The reason for this is unclear, but these residues are highly conserved among TAAs (Shahid *et al.*, 2012a) and a substitution to proline might drastically affect their, as-yet-unknown, function.

The gel analysis in Figure 3 shows that all the 'ASSA' region mutants are oligomers and behave similarly. As all four 'ASSA' region mutants have a similar apparent molecular weight, all further studies were performed with one representative mutant, $YadAM_{A354P}$. $YadAM_{wt}$ shows extreme stability towards heat and urea (Figure 4A) (Wollmann *et al.*, 2006), while $YadAM_{A354P}$ shows reduced stability towards thermal denaturation, as shown in Figure 4B. It should be noted, however, that it is still considerably more SDS-stable than the average protein oligomer. A minor band appears at around 20 kDa after heating, and can be interpreted as either a proteolysis product or a dimer, as claimed by Sikdar et al. (2017). This is further discussed below. $YadAM_{A354P}$ denatures into monomers after 4-6 min of heating at 85 °C with 4 M urea, whereas $YadAM_{wt}$ does not completely disintegrate into monomers, even after 4 h of heating under same conditions.

The $YadAM_{A354P}$ mutant is properly inserted into the outer membrane

Urea extraction was performed to address whether the decreased stability of $YadAM_{A354P}$ affected membrane insertion. In this experiment, the OM fractions are treated with urea, a chaotropic

reagent that denatures soluble proteins, but leaves the membrane bilayer and inserted proteins intact (Leo *et al.*, 2015b). If a protein is only loosely attached to the membrane, the urea will extract it, and after centrifugation, it will be found in the supernatant fraction. If a protein is properly inserted, it will be unaffected by the urea and remain in the pellet fraction. Like $YadAM_{wt}$, the $YadAM_{A354P}$ mutant was found in the pellet fraction after urea extraction, indicating that it is well inserted in the membrane (Figure 5).

$YadAM_{A354P}$ has reduced α-helical content

Secondary structure analysis of $YadAM_{wt}$ and $YadAM_{A354P}$ was performed using FTIR spectroscopy. An overlay of the second derivative spectra of both proteins shows that the peak corresponding to the α-helical signal is reduced in $YadAM_{A354P}$ compared to $YadAM_{wt}$, whereas the β-sheet signal peak is similar in both the mutant and wild-type proteins (Figure 6A). Calculation of the α-helical and β-sheet content of each provided an estimate of the reduced α-helical content in the $YadAM_{A354P}$ mutant, which is about 30% less compared with $YadAM_{wt}$ (Figure 6B). Since the β-sheet content is comparable, we conclude that the conformation of the β-barrel domain is mostly unaffected by the point mutation. For the helices, there are two possible explanations: either they are partially unfolded, or we observe a mix of two or more conformers, one with a secondary structure content close to the wildtype, and one where the helices are not formed at all or to only a very small extent.

The $YadA_{A354P}$ mutant neither forms lollipop-like surface structures nor autoaggregates

Full-length $YadA_{wt}$ shows lollipop-like projections on the surface of bacteria (Hoiczyk *et al.*, 2000). To study the effect of the proline substitution on surface exposure and fiber architecture of YadA, the A354P mutation was introduced into full-length $YadA_{wt}$. Electron micrographs of full-length $YadA_{wt}$ and $YadA_{A354P}$ expressed in *E. coli* show that, unlike the wildtype, $YadA_{A354P}$ is unable to form lollipop-shaped surface projections on the bacterial surface (Figure 7A and 7B). However, it is interesting to note that $YadA_{A354P}$ can be labeled to some extent with anti-YadA polyclonal antibody despite missing a fiber-like architecture (Figure 7B). The antibody labelling appears to be closer to the surface in the proline mutant when compared to $YadA_{wt}$, suggesting a collapsed structure. Overall labelling efficiency seemed to be reduced, presumably due to less

protein exposed on the cell surface compared to $YadA_{wt}$, but quantification was difficult, and led us to perform fluorescence-based assays (see below).

'Zipper-like' formations between $YadA_{wt}$ expressing cells were noticed in the electron micrographs, whereas these structures were absent in cells expressing $YadA_{A354P}$ (Figure 7C and 7D). The zipper structures are formed by the tips of the adhesin and are typical for autoaggregating TAAs (Hoiczyk *et al.*, 2000, Leo *et al.*, 2011). $YadA_{wt}$-expressing cells have the ability to autoaggregate, but the $YadA_{A354P}$ mutant seems to have lost its autoaggregation function. To confirm this, an autoaggregation assay was performed. If autoaggregation occurs, absorbance of an undisturbed culture decreases quickly as the aggregates sediment in the culture tube. This was the case for the cells expressing $YadA_{wt}$, but not for $YadA_{A354P}$ (Figure 8A). This was also clearly noticeable upon visual inspection of the tubes after 2 hours of static incubation. Cells expressing $YadA_{wt}$ had sedimented at the base of the tube, whereas the *E.coli* culture expressing $YadA_{A354P}$ appeared turbid (Figure 8B).

$YadA_{A354P}$ and $YadAM_{A354P}$ show reduced surface exposure and exist in two different conformations.

The above experiments indicate that $YadA_{A354P}$ is impaired structurally and functionally. Next, we wanted to check if the mutation also affects the translocation of the YadA passenger directly. To answer this question, the Spytag-SpyCatcher system (Zakeri *et al.*, 2012) was adapted. The Spytag is a specific 13-amino acid sequence which can spontaneously form a covalent isopeptide bond with a 16 kDa protein called SpyCatcher. $SpyCatcher_{EQ}$ is a variant of SpyCatcher (hereafter $SpyCatcher_{wt}$) which cannot form the isopeptide bond with a Spytag due to a point mutation in its active site and thus serves as a negative control. An N-terminal Spytag was introduced in $YadAM_{wt}$, $YadAM_{A354P}$, $YadA_{wt}$ and $YadA_{A354P}$ (see Figure 9A for exact position of the Spytag in each construct). For this assay, sfGFP-fused SpyCatcher ($SpyCatcher_{wt}$-sfGFP and $SpyCatcher_{Eq}$-sfGFP) were used, which allowed convenient detection and quantification of the amount of SpyCatcher bound to Spytagged proteins. *E. coli* cells expressing YadA constructs were treated with purified $SpyCatcher_{wt}$-sfGFP protein. If the Spytag was exposed on the surface, then $Spycatcher_{wt}$- sfGFP would bind to it and the cells would become fluorescent (Figure 9B), whereas if the passenger were stalled in a hairpin conformation with its N-termini facing the periplasm, or alternatively if the passenger never enters the barrel, then the Spytag cannot be accessed by the

extracellular SpyCatcher$_{wt}$-sfGFP and the cells are not fluorescent (Figure 9C). We used BL21-Gold(DE3) for these experiments, as we noticed that the OM integrity of the BL21ΔABCF strain was compromised and allowed some SpyCatcher to enter the periplasm (data not shown).

Indirect quantification of the amount of surface-exposed protein was done by measuring the fluorescence of bound SpyCatcher$_{wt}$-sfGFP using a plate reader at 533nm. In our experiments, SpyCatcher$_{wt}$-sfGFP bound to both, cells expressing YadAM$_{A354P}$ or full-length YadA$_{A354P}$, but in both cases, the total fluorescence was significantly reduced compared to cells expressing the corresponding wild-type proteins (YadAM$_{wt}$ and YadA$_{wt}$). For cells expressing YadAM$_{A354P}$ (Figure 10A) the fluorescence was reduced by 25% compared to YadAM$_{wt}$, though this is not a significant result in a rigorous statistical test. However, for the cells expressing YadA$_{A354P}$ (Figure 10B) the fluorescence was significantly reduced compared to YadA$_{wt}$, almost to background levels of the vector control.

The reduced fluorescence in this experiment suggests that a reduced amount of the YadAM$_{A354P}$ passenger domain is surface-exposed (translocated) compared to YadAM$_{wt}$. To check whether this is due to reduced overall expression levels, we performed quantitative SDS-PAGE of OM preparations for both YadAM$_{wt}$ and YadAM$_{A354P}$ (Figure 10C), confirming that expression levels between them are the same, and that differences in fluorescence intensity can thus be attributed to binding differences between fluorescent SpyCatcher to the Spytag in YadAM$_{wt}$ and YadAM$_{A354P}$. Unfortunately, a similar quantitative analysis is not easily performed for the full-length constructs, as wild-type YadA causes autoaggregation and clumping of the OM preparation, making reproducible quantification impossible. Figure 10D shows samples from these preparations. YadA trimers typically run as ladders of high molecular weight around 150 kDa on semi-native SDS gels (Grosskinsky *et al.*, 2007). Note the overall reduced amount of trimeric YadA$_{A354P}$ compared to trimeric wildtype YadA$_{wt}$ in Figure 10D – in line with published results of other transport-impaired mutant variants of YadA (Grosskinsky *et al.*, 2007), this strongly suggests degradation of the trimerized mutant protein during or after membrane insertion. The monomer bands of wildtype and mutant protein at 55 kDa are of comparable intensity and probably represent protein before trimerization and membrane insertion. The lack of trimeric protein for YadA$_{A354P}$ explains also why there is almost no surface labeling visible in panel 10B (compared to background controls),

and why there are not enough $YadA_{A354P}$ fibers present on the cell surface in Figure 7 to maintain a distance between cells comparable to the wildtype situation.

In conclusion, the reduced fluorescence of the (short) $YadAM_{A354P}$ construct compared to $YadAM_{wt}$ suggests multiple conformations of the mutant protein in the outer membrane. For the full-length constructs, this is impossible to assess as the protein is mostly degraded during or after membrane insertion.

$YadAM_{A354P}$ is trimeric

The Spytag-SpyCatcher assay can also be used to assess oligomerization state of the $YadAM_{A354P}$ and $YadA_{A354P}$ mutants. $YadA_{wt}$ is trimeric (Shahid *et al.*, 2012a), and consequently the Spytagged $YadA_{wt}$ displays three Spytags, which in turn can bind up to three SpyCatcher molecules. We expressed the short membrane anchor proteins $YadAM_{wt}$ and $YadAM_{A354P}$ in *E. coli* BL21-Gold(DE3) and treated them with $SpyCatcher_{wt}$-sfGFP. After separation with semi-native SDS-PAGE, and when visualizing $SpyCatcher_{wt}$-sfGFP-bound protein with a fluorescent imager, multiple bands are observed for the wild-type protein. Under non-saturating conditions, three bands were visible corresponding to one, two, and three $SpyCatcher_{wt}$-sfGFP labels (data not shown). We were not fully able to saturate the triple-labeled variant, but when using excess label, two bands are observed for the wild type (Figure 11), corresponding to two and three bound SpyCatcher proteins per trimer, and with the majority of the trimers triple-labeled based on relative intensities of the fluorescent bands. Under the same labeling conditions, the proline mutant shows three bands, corresponding to one to three bound SpyCatcher molecules (Figure 11), providing clear evidence that $YadAM_{A354P}$ is indeed a trimer despite the difference in migration behavior compared with the wildtype. Additionally, a fourth band corresponding to free $SpyCatcher_{wt}$-sfGFP is visible in the proline mutant lanes. The $YadAM_{A354P}$ mutant shows different relative intensities in the labeling pattern, with the band corresponding to two bound SpyCatcher molecules visibly stronger than the bands corresponding to one and three bound SpyCatchers. The apparent lower overall fluorescence intensity (note that expression levels are identical, see figure 10) prompted us to look for an additional, unlabeled trimer band in the mutant sample. This extra band is apparent in the right panel in Figure 11 only for the mutant protein after Coomassie staining. For better visualization, the same samples were also applied to a 4-12% gradient SDS-PAGE gel, providing better separation at a broader weight range. A strong band was identified at ~26 kDa (see supplementary

Figure S1), which corresponds to the unlabeled oligomer of $YadAM_{A354P}$ (see also Figure 3). This band was confirmed by mass spectrometry to consist of unlabeled $YadAM_{A354P}$, showing that the majority of the fully formed $YadAM_{A354P}$ passenger domains are not exported, while they are still properly inserted in the membrane in trimeric form. A small amount of unlabeled trimer is also visible for the wildtype ($YadAM_{wt}$), but in this case, the majority of protein can be fully labeled with three labels. Note that when the cells are lysed, labelling patterns change for the $YadAM_{A354P}$ mutant as the periplasmically located Spytags are then exposed to the SpyCatcher protein. The wild-type protein $YadAM_{wt}$ cannot be labeled any more in the lysis experiment, suggesting that the main reason for incomplete labeling in this case is steric hindrance.

To examine the effect of the mutation on the export of full-length YadA, $YadA_{wt}$ and $YadA_{A354P}$ were treated with SpyCatcher-sfGFP in an identical experiment. Several technical issues prohibited a detailed analysis of this experiment. $YadA_{wt}$ is known to already display ladder-like SDS-PAGE migration behavior without any additional labeling (Grosskinsky *et al.*, 2007), and after fluorescent labelling, the resulting band patterns were difficult to interpret. In addition, the samples of $YadA_{A354P}$ very clearly contained significantly less trimeric protein (see also Figure 10D) and were hard to detect at all in the fluorescent images (in accordance with the plate reader results, Figure 10). When loading large amounts of the $YadA_{A354P}$ sample, the gels became smeary due to excess membrane lipids and again difficult to image.

Periplasmic SpyTag is not accessible to SpyCatcher-sfGFP added externally

To demonstrate that periplasmically located SpyTag is not accessible to externally added SpyCatcher, we produced a periplasmically located SpyTag-MBP fusion. A Western blot using an anti-MBP antibody (Figure 12) shows that SpyCatcher only reacts with MBP from lysed cells, demonstrating that SpyCatcher-sfGFP is not able to penetrate into the periplasm. The samples contain both pre-MBP (with signal peptide) and periplasmic MBP. SpyTag-MBP forms a covalent bond with SpyCatcher-sfGFP to the extent that the 43 kDa band in the unwashed sample is significantly weaker than in the washed sample, since most of it is sequestered in the 85 kDa band

representing MBP-SpyCatcher-sfGFP. This experiment demonstrates that SpyCatcher-sfGFP does not cross an intact outer membrane.

In a final control experiment, we tried to express SpyCatcher in the periplasm with the help of a signal peptide. When co-expressing this construct with wither $YadA_{wt}$/$YadA_{A354}$ or $YadA_{wt}$/$YadA_{A354P}$, this should in principle lead to specific labeling only of the fraction of SpyTag that remains in the periplasm after membrane insertion. The results were inconclusive: we were able to show that periplasmic SpyCatcher leaked into the extracellular space, and that labelling in the periplasm also in part occurred even before membrane insertion of the constructs, leading to increased levels of labeled monomers, and to partial proteolysis of the samples in some cases (see supplementary Figure S2). We conclude that the SpyCatcher assay is a powerful tool to assess surface localization of translocated proteins, but it is not expedient for capture of transient periplasmic intermediates, mainly due to high labeling background.

Discussion

The hairpin model for passenger translocation is established for Type Va and Ve secretion systems, but direct experimental evidence has been lacking for Type Vc secretion until now. In our model protein, the trimeric autotransporter adhesin YadA, a single proline substitution in the presumed hairpin-initiating region had dramatic effects on surface display, trimer stability, and overall protein function, both for constructs comprising of only the membrane anchor domain and full-length constructs that include the complete passenger.

In a recent publication, Sikdar et al. described asymmetric trimers of another TAA, UpaG, when applying site-specific crosslinking to capture membrane insertion intermediates (Sikdar *et al.*, 2017). In this work, the authors observed an apparent molecular weight of an oligomer that corresponds to a dimer. They interpreted this as the loss of one of the three monomers during electrophoresis or SDS sample preparation, and concluded that one of the monomers is easier to remove than the rest. Their experimental system lead them to suggest periplasmic, trimeric intermediates of membrane insertion that are not symmetrical. While this is entirely possible, our results from a related TAA, YadA, do not support a dimer intermediate at any stage that we can capture in our experiments. We do observe unusual migration behavior of our proteins, and

specifically of the proline mutants in our study, but our fluorescence labeling results very clearly demonstrate that the protein is a stable trimer at all times, also during electrophoresis. Note though that in the mutant $YadAM_{A354P}$ in Figure 4 after heating, something that might be interpreted as a minor dimer band is visible in addition to trimer and monomer bands. Our point mutations capture a later insertion intermediate compared to the work of Sikdar et al. – YadA is already fully inserted in the membrane in our experiments. The trimeric intermediates are further corroborated by urea extraction assays that confirmed proper membrane insertion of the trimers, and by FTIR experiments that show comparable β-sheet content of $YadAM_{wt}$ and $YadAM_{A354P}$, while there was a reduction in the α-helical content of $YadAM_{A354P}$. This clearly indicates that the barrel is similar, while the proline mutation affects the helical part residing within the β-barrel, leading to the conformational changes that prohibit proper surface display of the passenger. Note that the FTIR measurements cannot distinguish between a situation where all trimers are the same, or exist in a mix of two or more conformations.

We do observe a certain level of potential asymmetry in the labeling experiments for $YadAM_{A354P}$, and to a smaller extent for $YadAM_{wt}$. A relatively small fraction of the wild-type trimers cannot be saturated with three SpyCatcher molecules, and for the mutant, we observe variants with two and with one label only, even though the major fraction of $YadAM_{A354P}$ is not labeled at all (Figure 11, and supplementary materials). It is worth noting that upon cell lysis, SpyCatcher can also label Spytags that were previously shielded in the periplasm. In our hands, the wild-type protein cannot be labeled further, but the mutant protein $YadAM_{A354P}$ changes its fluorescent band pattern strongly in this situation.

Incomplete labeling of the wildtype can probably be explained by steric hindrance and the resulting kinetic effects that do not allow for full saturation of the label. The existence of asymmetric conformers in the proline mutant variants is strongly suggested by the fluorescent labeling behavior of $YadAM_{A354P}$. The proline mutation is clearly disruptive to the autotransport process, at a time point where the β-barrel trimers are fully formed and inserted in the outer membrane – shown by urea extraction experiments, and by FTIR data that corroborates the same beta-sheet content for wildtype and mutant protein. In the full-length construct $YadA_{A354P}$, the disruptive mutation leads to what we interpret as downstream degradation after insertion, very similar to what was observed earlier for other point mutations of a conserved glycine residue in the barrel wall that disrupt

autotransport in YadA (Grosskinsky *et al.*, 2007). In that study, deletion of the periplasmic protease DegP restored surface display of YadA almost completely. The data from YadAM$_{A354P}$ strongly suggests that the passenger must be exported through the pore, as has been shown for other classes of autotransporters – because we do find parts of the passenger localized in the periplasm while the translocation barrel is already formed.

It is highly improbable that TAAs would be exported through their own autotransport pore in an asymmetric mechanism. The extracellular domains of TAAs that are more complex than YadA are highly intertwined (Bassler *et al.*, 2015), and are not stable as monomers. An asymmetric export mechanism would require coordinated folding, and the current model is that this folding has to proceed in a concerted, zipper-like fashion from C- to N-terminus. In some cases, it appears possible to export single TAA chains, e.g. when fused to the translocator of a classical autotransporter or when a TAA with a truncated passenger is co-expressed with the corresponding full-length protein (Surana *et al.*, 2004, Cotter *et al.*, 2006, Cugini *et al.*, 2018). However, in these cases the resulting protein had lost most of the adhesive capability of the native trimeric protein, indicating that single TAA chains do not fold correctly. The fact that complex TAAs, such as *Salmonella* SadA, require trimeric helper proteins in the periplasm for efficient surface display supports this notion of concerted export and folding (Grin *et al.*, 2014). However, it is conceivable that locally and temporarily, asymmetry exists and needs to be resolved for wild-type TAAs during export of the passenger, and that our proline mutant variants are to some extent locked in such asymmetric states. It is also possible that we capture mixed trimers with some strands exported and some remaining in the periplasm based solely on the fact that proline exists in two rigid conformations, cis and trans, that cannot be converted from one to the other without breaking a covalent bond.

In conclusion, our results suggest that the trimeric ATs translocate their passenger domain via a hairpin intermediate through a pore, just like their type Va and Ve secretion system counterparts. The ‘ASSA’ region is a flexible stretch in the transmembrane α-helix of YadA which plays an important role in forming the temporary hairpin structure during the autotransport process in this model. By introducing single proline substitutions in the ‘ASSA’ region we have obtained multiple conformers of the mutants, with the most abundant conformer being one where all three passenger chains remain in the periplasm and are occluded from extracellular labels. We are currently

investigating whether it is feasible to study the mixed conformers in solid-state NMR experiments in order to obtain a high-resolution structure of this stalled transport intermediate, and to obtain information on the conformation of the proline residues that we introduced.

Acknowledgements:

We thank Han Remaut, Finn Aachmann, and Harris Bernstein for critical discussions. This work was funded by grants from the Norwegian Research Council to DL, MOR, and JCL, and by institutional funds from the University of Oslo.

The constructs for SpyCatcher assays were deposited with AddGene (107420 pIBA3-SpyCatcher-sfGFP, 107421 pIBA3-SpyCatcher$_{EQ}$-sfGPF, 107422 pIBA2-SpyTag-MBP)

Figure Legends

Figure 1: Schematic representation of the hairpin model of passenger translocation in Type Va and Type Ve autotransporters. The β-barrel is formed with the help of BAM complex. The passenger chain proximal to the barrel loops in to the pore of barrel forming a hairpin structure. As the passenger emerges on the extracellular surface it starts to fold and pulls the rest of the passenger chain to the outside of the cell through the barrel lumen.

Figure 2: **(A)** A computational model structure of full length YadA consisting of the C-terminal β-barrel domain, the coiled-coil stalk domain and the N-terminal head domain (Koretke *et al.*, 2006). **(B)** The structure of the membrane anchor domain of YadA (Protein Data Base id: 2LME, solved by solid-state NMR) which consists of the C-terminal β-barrel domain and a small part of the passenger. The unstructured N-terminal part of the structure originates from an N-terminal Strep tag. **(C)** A part of the membrane anchor domain of YadA which highlights the 'ASSA' region (red), a stretch of flexible residues located in the transmembrane part of the passenger domain (Shahid *et al.*, 2012a). The sequence corresponding to the membrane anchor domain construct of YadA (YadAM) used in this study is given in the insert. The ASSA region is highlighted in red and the Strep tag in pink.

Figure 3: Silver stained SDS-PAGE gel containing outer membrane preparations of $YadAM_{G352P}$, $YadAM_{L353P}$, $YadAM_{A354P}$, $YadAM_{S355P}$, $YadAM_{S356P}$, $YadAM_{A357P}$, $YadAM_{A358P}$, $YadAM_{L359P}$, $YadAM_{wt}$ (wt), and pASK-IBA2 vector control (vc) from left to right. The bands corresponding to the YadA variant are boxed. All four ASSA region mutants (i.e. $YadAM_{A354P}$, $YadAM_{S355P}$, $YadAM_{S356P}$, $YadAM_{A357P}$) run at the same size, around 26 kDa, while $YadAM_{L353P}$ and $YadAM_{A358P}$ have a higher apparent molecular weight compared to the ASSA region mutants, but still lower than $YadAM_{wt}$ which runs at 45 kDa (Wollmann *et al.*, 2006). $YadAM_{L359P}$ was not expressed at all, while $YadAM_{G358P}$ expression is barely visible.

Figure 4: Stability assay of outer membrane preparations of membrane anchor domains of **(A)** $YadAM_{wt}$ and **(B)** $YadAM_{A354P}$. The samples were treated with 4 M urea and heated at 85 ˚C for the indicated time. L- Protein marker and U- unheated samples.

Figure 5: Urea extraction of $YadAM_{wt}$ and $YadAM_{A354P}$. The outer membrane fractions were treated with 6 M urea for an hour followed by ultracentrifugation. Both the $YadAM_{wt}$ and $YadAM_{A354P}$ proteins are found in the pellet fraction following extraction, and the apparent molecular weights remain unchanged compared to Figure 3. L - Protein marker, S - Supernatant and P - Pellet.

Figure 6: FTIR analysis data of $YadAM_{wt}$ and $YadAM_{A354P}$. **(A)** Overlay of the second derivative spectra of $YadAM_{wt}$ (blue) and $YadAM_{A354P}$ (red). Peaks representing the α-helix and β-sheet signals are marked by arrows. **(B)** The table shows the secondary structure content as well as protein concentration of $YadAM_{wt}$ and $YadAM_{A354P}$, calculated using the FTIR data analysis software from Bruker Optics.

Figure 7: Electron micrographs of cross-sections of immunogold-labelled $YadA_{wt}$ **(A)** and $YadA_{A354P}$ **(B)** expressed in *E. coli*. Lollipop-shaped surface projections are seen on the surface of wild type expressing cells, but are missing in the cells expressing the proline mutant **,** while the gold labelling is present in both (indicated by black arrows). 'Zipper-like' formations promoting autoaggregation are observed in *E.coli* expressing $YadA_{wt}$ **(C)** (indicated by a black arrows) but missing in *E.coli* expressing $YadA_{A354P}$ **(D)**.

Figure 8: Effect of **(A)** The turbidity of cultures expressing $YadA_{wt}$, $YadA_{A354P}$ and empty vector control was measured every 20 min after 2 h of expression. The OD_{600} of $YadA_{wt}$ expressing cells

decreases whereas that of $YadA_{A354P}$ and empty vector (pASK-IBA2) control is comparable and stays more or less constant with time. **(B)** Cultures expressing $YadA_{wt}$ (left) and $YadA_{A354P}$ (right) after 2 h of static incubation.

Figure 9: Schematic representation of the Spytag-SpyCatcher assay. **(A)** A Spytag was introduced between the signal peptide and full-length $YadA_{wt}$ and $YadA_{A354P}$ sequence. In the $YadAM_{wt}$ and $YadAM_{A354P}$ construct, a Spytag was introduced between the Strep tag and the YadAM sequence. The exact positions are marked with arrows. The numbering corresponds to the YadA sequence from *Y. enterocolitica* WA-314 (GenBank YP_006960953). **(B)** If the N-termini of YadA are exposed on the cell surface, binding of SpyCatcher molecules to exposed Spytags would make the cell fluorescent. **(C)** If the N-termini are facing the periplasm then SpyCatcher is unable to bind to Spytag and the cell will not be fluorescent. Orange squares represent Spytags, Green circles represent SpyCatcher-sfGFP. Note that possible asymmetric conformers are ignored in this schematic for simplicity.

Figure 10: Fluorescence measurement of $SpyCatcher_{wt}$-sfGFP-treated samples using a plate reader. **A**: control (pASK-IBA2), $YadAM_{wt}$ and $YadAM_{A354P}$ expressed in *E. coli* BL21-Gold(DE3). **B**: empty vector control (pASK-IBA2), full-length $YadA_{wt}$ and $YadA_{A354P}$ expressed in *E. coli* BL21-Gold(DE3). Statistical analysis was performed using a two-tailed ANOVA followed by Tukey's multiple comparison test using GraphPad Prism. 3 stars signify a p-value of less than 0.001, and n.s. signifies "non-significant" ($p > 0.05$). **C**: SDS-PAGE of OM preparations for BL21ΔABCF containing the empty vector control, $YadAM_{wt}$, and $YadAM_{A354P}$. Note that the bands in the gel correspond to fully urea-denatured monomer and thus do not display a size difference between wild-type and mutant proteins. The raw densitometry values are given below the gel bands. **D**: SDS-PAGE of enriched OM preparation of full length YadA and $YadA_{A354P}$ and empty vector control. Significantly lower amounts of trimerized $YadA_{A354P}$ is observed compared to the wild type. However, roughly the same amount of pre-insertion monomer (around 55 kDa) is observed in both samples, indicating that both constructs have similar expression levels, but that $YadA_{A354P}$ upon insertion is proteolytically degraded (see text).

Figure 11: $SpyCatcher_{wt}$-sfGFP assay of lysed and unlysed cells expressing $YadAM_{wt}$, $YadAM_{A354P}$, and pASK-IBA2 (pIBA2) as the vector control (vc). For the unlysed samples, excess label was washed away before sample SDS-PAGE sample preparation, while the lysed samples

included the excess label during the whole process, enabling full labeling of Spy tags that were otherwise masked in the periplasm. The gels are visualized by blue light (left) to excite fluorescence, and stained with Coomassie R-250 (right) for size comparison. A ladder-like pattern of up to three bands, corresponding to assembled trimers bound to 1-3 SpyCatcher$_{wt}$-sfGFPmolecules is observed in all samples in the fluorescent gel (approximate sizes are 67, 109, and 150 kDa. Marked with white arrows). An additional green band is visible in the YadAM$_{A354P}$ samples, thought to represent unreacted SpyCatcher$_{wt}$-sfGFP(41.3 kDa). YadAM$_{wt}$ displays a similar intensity pattern in both lysed and unlysed samples, with the most intense band corresponding to three bound SpyCatcher$_{wt}$-sfGFP molecules, and a weaker band corresponding to two bound molecules, indicating that YadAM$_{wt}$ presents three Spy-tagged strands on the bacterial surface for reacting with the SpyCatcher$_{wt}$-sfGFP molecules. The lysed and unlysed YadAM$_{A354P}$ samples all have three bands, but differ with regards to the intensity pattern. The strongest band in the unlysed sample corresponds to two bound SpyCatcher$_{wt}$-sfGFP molecules, while this changes to 3 bound molecules in the lysed sample, indicating that lysing the bacteria increase the SpyCatcher$_{wt}$-sfGFP access to the YadAM$_{A354P}$ N-termini. An extra band visible in the YadA$_{A354P}$ samples in the stained gel, at around 27 kDa, was suspected to correspond to unreacted YadA$_{A354P}$. This was confirmed by separating the unlysed samples on a gradient SDS-PAGE gel and excising the band for mass spectrometry (See Supplementary figure 1).

Figure 12: Binding of SpyCatcher$_{wt}$-sfGFP to periplasmic MBP

Western blot of SpyTag-MBP expressing bacteria probed with an anti-MalE antibody. Bacteria expressing periplasmic SpyTag-MBP were incubated with extracellular SpyCatcher$_{wt}$-sfGFP (Spy). The cells were either washed (W) or left unwashed (U) before cell lysis. Thus, the unwashed cells were lysed in the presence of SpyCatcher$_{wt}$-sfGP, whereas washing the cells removed it. The supernatant from the lysed samples was subjected to SDS-PAGE and then transferred to a nitrocellulose membrane. The membrane was probed with an anti-MalE antibody and detected using near-infrared fluorescence. As controls, we included the empty vector (pASK-IBA2) and the non-reactive variant SpyCatcher$_{EQ}$-sfGFP (EQ). The SpyTag-MBP expressing samples contain both pre-MBP and mature MBP; expected size of the latter is 43 kDa. The expected size for the MBP-SpyCatcher-sfGFP complex is 84 kDa.

References

Adams, T.M., Wentzel, A., and Kolmar, H. (2005) Intimin-mediated export of passenger proteins requires maintenance of a translocation-competent conformation. *J Bacteriol* **187**: 522-533.

Alvarez, B.H., Gruber, M., Ursinus, A., Dunin-Horkawicz, S., Lupas, A.N., and Zeth, K. (2010) A transition from strong right-handed to canonical left-handed supercoiling in a conserved coiled-coil segment of trimeric autotransporter adhesins. *J Struct Biol* **170**: 236-245.

Bakelar, J., Buchanan, S.K., and Noinaj, N. (2016) The structure of the beta-barrel assembly machinery complex. *Science* **351**: 180-186.

Bassler, J., Hernandez Alvarez, B., Hartmann, M.D., and Lupas, A.N. (2015) A domain dictionary of trimeric autotransporter adhesins. *Int J Med Microbiol* **305**: 265-275.

Byrappa, S., Gavin, D.K., and Gupta, K.C. (1995) A highly efficient procedure for site-specific mutagenesis of full-length plasmids using Vent DNA polymerase. *Genome Res* **5**: 404-407.

Cotter, S.E., Surana, N.K., Grass, S., and St Geme, J.W., 3rd (2006) Trimeric autotransporters require trimerization of the passenger domain for stability and adhesive activity. *J Bacteriol* **188**: 5400-5407.

Cugini, C., Mei, Y., Furgang, D., George, N., Ramasubbu, N., and Fine, D.H. (2018) Utilization of Variant and Fusion Proteins To Functionally Map the Aggregatibacter actinomycetemcomitans Trimeric Autotransporter Protein ApiA. *Infect Immun* **86**.

Drobnak, I., Braselmann, E., and Clark, P.L. (2015) Multiple driving forces required for efficient secretion of autotransporter virulence proteins. *J Biol Chem* **290**: 10104-10116.

Fan, E., Chauhan, N., Udatha, D.B., Leo, J.C., and Linke, D. (2016) Type V Secretion Systems in Bacteria. *Microbiol Spectr* **4**.

Gibson, D.G., Young, L., Chuang, R.Y., Venter, J.C., Hutchison, C.A., 3rd, and Smith, H.O. (2009) Enzymatic assembly of DNA molecules up to several hundred kilobases. *Nat Methods* **6**: 343-345.

Grin, I., Hartmann, M.D., Sauer, G., Hernandez Alvarez, B., Schutz, M., Wagner, S., Madlung, J., Macek, B., Felipe-Lopez, A., Hensel, M., Lupas, A., and Linke, D. (2014) A trimeric lipoprotein assists in trimeric autotransporter biogenesis in enterobacteria. *J Biol Chem* **289**: 7388-7398.

Grin, I., Schwarz, H., and Linke, D. (2011) Electron microscopy techniques to study bacterial adhesion. *Adv Exp Med Biol* **715**: 257-269.

Grosskinsky, U., Schutz, M., Fritz, M., Schmid, Y., Lamparter, M.C., Szczesny, P., Lupas, A.N., Autenrieth, I.B., and Linke, D. (2007) A conserved glycine residue of trimeric autotransporter domains plays a key role in Yersinia adhesin A autotransport. *J Bacteriol* **189**: 9011-9019.

Hartmann, M.D., Grin, I., Dunin-Horkawicz, S., Deiss, S., Linke, D., Lupas, A.N., and Alvarez, B.H. (2012) Complete fiber structures of complex trimeric autotransporter adhesins conserved in enterobacteria. *Proceedings of the National Academy of Sciences of the United States of America* **109**: 20907-20912.

Hoiczyk, E., Roggenkamp, A., Reichenbecher, M., Lupas, A., and Heesemann, J. (2000) Structure and sequence analysis of Yersinia YadA and Moraxella UspAs reveal a novel class of adhesins. *EMBO J* **19**: 5989-5999.

Holdbrook, D.A., Piggot, T.J., Sansom, M.S., and Khalid, S. (2013) Stability and membrane interactions of an autotransport protein: MD simulations of the Hia translocator domain in a complex membrane environment. *Biochim Biophys Acta* **1828**: 715-723.

Ieva, R., and Bernstein, H.D. (2009) Interaction of an autotransporter passenger domain with BamA during its translocation across the bacterial outer membrane. *Proc Natl Acad Sci U S A* **106**: 19120-19125.

Jeeves, M., and Knowles, T.J. (2015) A novel pathway for outer membrane protein biogenesis in Gram-negative bacteria. *Mol Microbiol* **97**: 607-611.

Junker, M., Besingi, R.N., and Clark, P.L. (2009) Vectorial transport and folding of an autotransporter virulence protein during outer membrane secretion. *Mol Microbiol* **71**: 1323-1332.

Koretke, K.K., Szczesny, P., Gruber, M., and Lupas, A.N. (2006) Model structure of the prototypical non-fimbrial adhesin YadA of Yersinia enterocolitica. *J Struct Biol* **155**: 154-161.

Lehr, U., Schutz, M., Oberhettinger, P., Ruiz-Perez, F., Donald, J.W., Palmer, T., Linke, D., Henderson, I.R., and Autenrieth, I.B. (2010) C-terminal amino acid residues of the trimeric autotransporter adhesin YadA of Yersinia enterocolitica are decisive for its recognition and assembly by BamA. *Mol Microbiol* **78**: 932-946.

Leo, J.C., Grin, I., and Linke, D. (2012) Type V secretion: mechanism(s) of autotransport through the bacterial outer membrane. *Philos Trans R Soc Lond B Biol Sci* **367**: 1088-1101.

Leo, J.C., Lyskowski, A., Hattula, K., Hartmann, M.D., Schwarz, H., Butcher, S.J., Linke, D., Lupas, A.N., and Goldman, A. (2011) The structure of E. coli IgG-binding protein D suggests a general model for bending and binding in trimeric autotransporter adhesins. *Structure* **19**: 1021-1030.

Leo, J.C., Oberhettinger, P., Chaubey, M., Schutz, M., Kuhner, D., Bertsche, U., Schwarz, H., Gotz, F., Autenrieth, I.B., Coles, M., and Linke, D. (2015a) The Intimin periplasmic domain mediates dimerisation and binding to peptidoglycan. *Mol Microbiol* **95**: 80-100.

Leo, J.C., Oberhettinger, P., and Linke, D. (2015b) Assessing the Outer Membrane Insertion and Folding of Multimeric Transmembrane beta-Barrel Proteins. *Methods Mol Biol* **1329**: 157-167.

Leo, J.C., Oberhettinger, P., Yoshimoto, S., Udatha, D.B., Morth, J.P., Schutz, M., Hori, K., and Linke, D. (2016) Secretion of the Intimin Passenger Domain Is Driven by Protein Folding. *J Biol Chem* **291**: 20096-20112.

Leyton, D.L., Sevastsyanovich, Y.R., Browning, D.F., Rossiter, A.E., Wells, T.J., Fitzpatrick, R.E., Overduin, M., Cunningham, A.F., and Henderson, I.R. (2011) Size and conformation limits to secretion of disulfide-bonded loops in autotransporter proteins. *J Biol Chem* **286**: 42283-42291.

Linke, D., Riess, T., Autenrieth, I.B., Lupas, A., and Kempf, V.A. (2006) Trimeric autotransporter adhesins: variable structure, common function. *Trends Microbiol* **14**: 264-270.

Meng, G., Surana, N.K., St Geme, J.W., 3rd, and Waksman, G. (2006) Structure of the outer membrane translocator domain of the Haemophilus influenzae Hia trimeric autotransporter. *EMBO J* **25**: 2297-2304.

Meuskens, I., Michalik, M., Chauhan, N., Linke, D., and Leo, J.C. (2017) A New Strain Collection for Improved Expression of Outer Membrane Proteins. *Front Cell Infect Microbiol* **7**: 464.

Mikula, K.M., Leo, J.C., Lyskowski, A., Kedracka-Krok, S., Pirog, A., and Goldman, A. (2012) The translocation domain in trimeric autotransporter adhesins is necessary and sufficient for trimerization and autotransportation. *J Bacteriol* **194**: 827-838.

Muhlenkamp, M., Oberhettinger, P., Leo, J.C., Linke, D., and Schutz, M.S. (2015) Yersinia adhesin A (YadA)--beauty & beast. *Int J Med Microbiol* **305**: 252-258.

Natale, P., Bruser, T., and Driessen, A.J. (2008) Sec- and Tat-mediated protein secretion across the bacterial cytoplasmic membrane--distinct translocases and mechanisms. *Biochim Biophys Acta* **1778**: 1735-1756.

Nesterenko, M.V., Tilley, M., and Upton, S.J. (1994) A simple modification of Blum's silver stain method allows for 30 minute detection of proteins in polyacrylamide gels. *J Biochem Biophys Methods* **28**: 239-242.

Nummelin, H., Merckel, M.C., Leo, J.C., Lankinen, H., Skurnik, M., and Goldman, A. (2004) The Yersinia adhesin YadA collagen-binding domain structure is a novel left-handed parallel beta-roll. *EMBO J* **23**: 701-711.

Oberhettinger, P., Leo, J.C., Linke, D., Autenrieth, I.B., and Schutz, M.S. (2015) The inverse autotransporter intimin exports its passenger domain via a hairpin intermediate. *J Biol Chem* **290**: 1837-1849.

Orwick-Rydmark, M., Arnold, T., and Linke, D. (2016) The Use of Detergents to Purify Membrane Proteins. *Curr Protoc Protein Sci* **84**: 4 8 1-4 8 35.

Plummer, A.M., and Fleming, K.G. (2016) From Chaperones to the Membrane with a BAM! *Trends Biochem Sci* **41**: 872-882.

Rath, A., Glibowicka, M., Nadeau, V.G., Chen, G., and Deber, C.M. (2009) Detergent binding explains anomalous SDS-PAGE migration of membrane proteins. *Proc Natl Acad Sci U S A* **106**: 1760-1765.

Roggenkamp, A., Ackermann, N., Jacobi, C.A., Truelzsch, K., Hoffmann, H., and Heesemann, J. (2003) Molecular analysis of transport and oligomerization of the Yersinia enterocolitica adhesin YadA. *J Bacteriol* **185**: 3735-3744.

Roman-Hernandez, G., Peterson, J.H., and Bernstein, H.D. (2014) Reconstitution of bacterial autotransporter assembly using purified components. *Elife* **3**: e04234.

Ruiz-Perez, F., Henderson, I.R., Leyton, D.L., Rossiter, A.E., Zhang, Y., and Nataro, J.P. (2009) Roles of periplasmic chaperone proteins in the biogenesis of serine protease autotransporters of Enterobacteriaceae. *J Bacteriol* **191**: 6571-6583.

Ruiz-Perez, F., Henderson, I.R., and Nataro, J.P. (2010) Interaction of FkpA, a peptidyl-prolyl cis/trans isomerase with EspP autotransporter protein. *Gut Microbes* **1**: 339-344.

Saragliadis, A., Trunk, T., and Leo, J.C. (2018) Producing Gene Deletions in Escherichia coli by P1 Transduction with Excisable Antibiotic Resistance Cassettes. *J Vis Exp*.

Sauri, A., Soprova, Z., Wickstrom, D., de Gier, J.W., Van der Schors, R.C., Smit, A.B., Jong, W.S., and Luirink, J. (2009) The Bam (Omp85) complex is involved in secretion of the autotransporter haemoglobin protease. *Microbiology* **155**: 3982-3991.

Schagger, H. (2006) Tricine-SDS-PAGE. *Nat Protoc* **1**: 16-22.

Shahid, S.A., Bardiaux, B., Franks, W.T., Krabben, L., Habeck, M., van Rossum, B.J., and Linke, D. (2012a) Membrane-protein structure determination by solid-state NMR spectroscopy of microcrystals. *Nat Methods* **9**: 1212-1217.

Shahid, S.A., Markovic, S., Linke, D., and van Rossum, B.J. (2012b) Assignment and secondary structure of the YadA membrane protein by solid-state MAS NMR. *Sci Rep* **2**: 803.

Sikdar, R., Peterson, J.H., Anderson, D.E., and Bernstein, H.D. (2017) Folding of a bacterial integral outer membrane protein is initiated in the periplasm. *Nat Commun* **8**: 1309.

Surana, N.K., Cutter, D., Barenkamp, S.J., and St Geme, J.W., 3rd (2004) The Haemophilus influenzae Hia autotransporter contains an unusually short trimeric translocator domain. *J Biol Chem* **279**: 14679-14685.

Szczesny, P., and Lupas, A. (2008) Domain annotation of trimeric autotransporter adhesins--daTAA. *Bioinformatics* **24**: 1251-1256.

Thanassi, D.G., Stathopoulos, C., Karkal, A., and Li, H. (2005) Protein secretion in the absence of ATP: the autotransporter, two-partner secretion and chaperone/usher pathways of gram-negative bacteria (review). *Mol Membr Biol* **22**: 63-72.

Wollmann, P., Zeth, K., Lupas, A.N., and Linke, D. (2006) Purification of the YadA membrane anchor for secondary structure analysis and crystallization. *Int J Biol Macromol* **39**: 3-9.

Yu, W., and Gotz, F. (2012) Cell wall antibiotics provoke accumulation of anchored mCherry in the cross wall of Staphylococcus aureus. *PLoS One* **7**: e30076.

Zakeri, B., Fierer, J.O., Celik, E., Chittock, E.C., Schwarz-Linek, U., Moy, V.T., and Howarth, M. (2012) Peptide tag forming a rapid covalent bond to a protein, through engineering a bacterial adhesin. *Proc Natl Acad Sci U S A* **109**: E690-697.

Zhang, W.B., Sun, F., Tirrell, D.A., and Arnold, F.H. (2013) Controlling macromolecular topology with genetically encoded SpyTag-SpyCatcher chemistry. *J Am Chem Soc* **135**: 13988-13997.

Figure 1

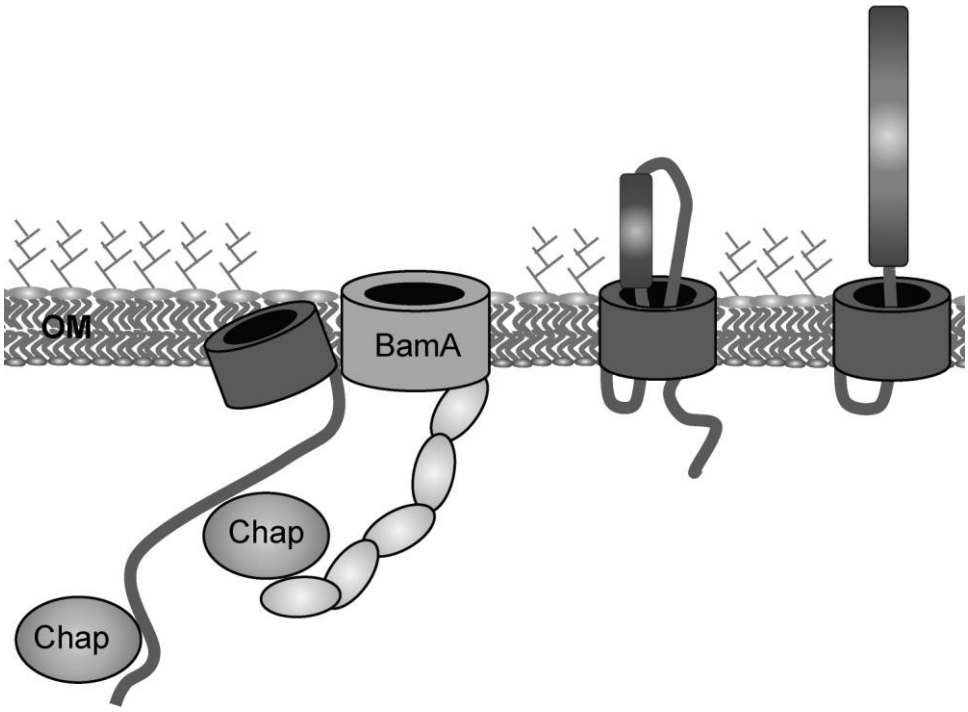

Figure 2

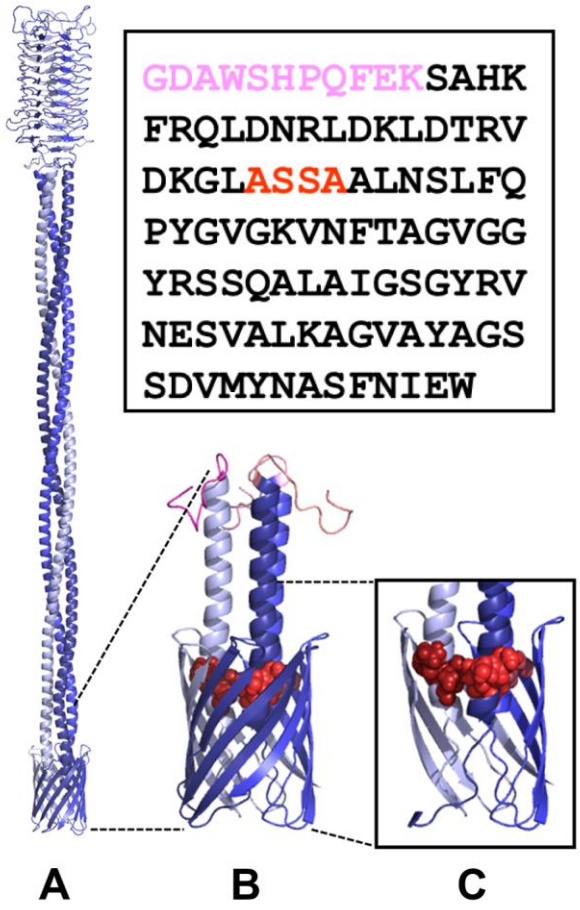
GDAWSHPQFEKSAHK
FRQLDNRLDKLDTRV
DKGLASSAALNSLFQ
PYGVGKVNFTAGVGG
YRSSQALAIGSGYRV
NESVALKAGVAYAGS
SDVMYNASFNIEW
A
B
C

Figure 3

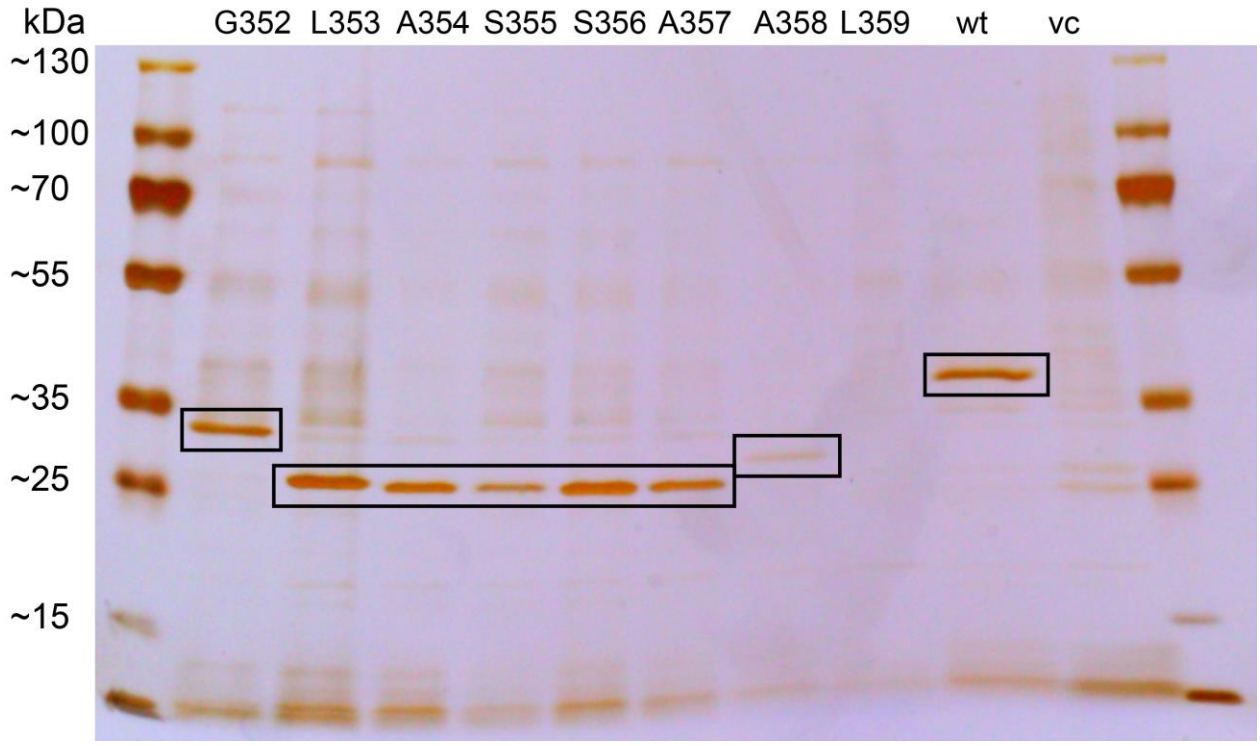

Figure 4

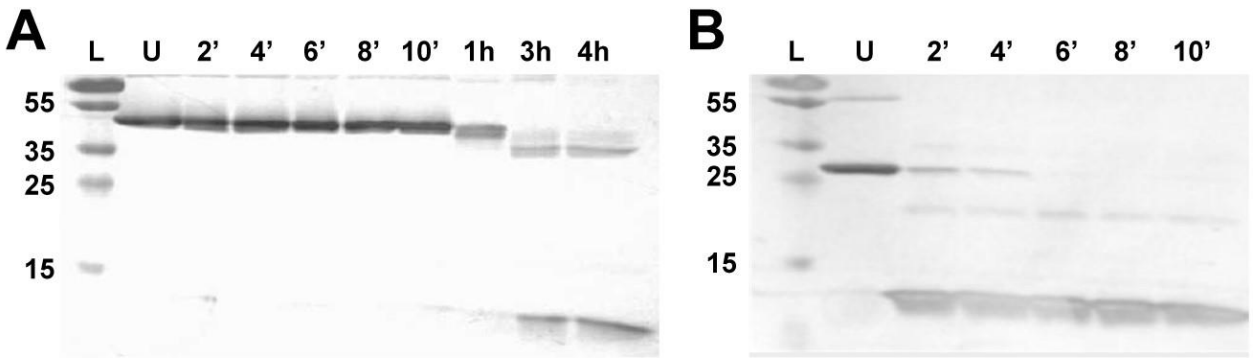

Figure 5

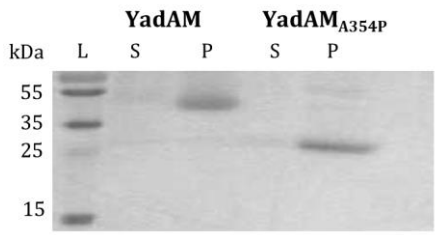

Figure 6

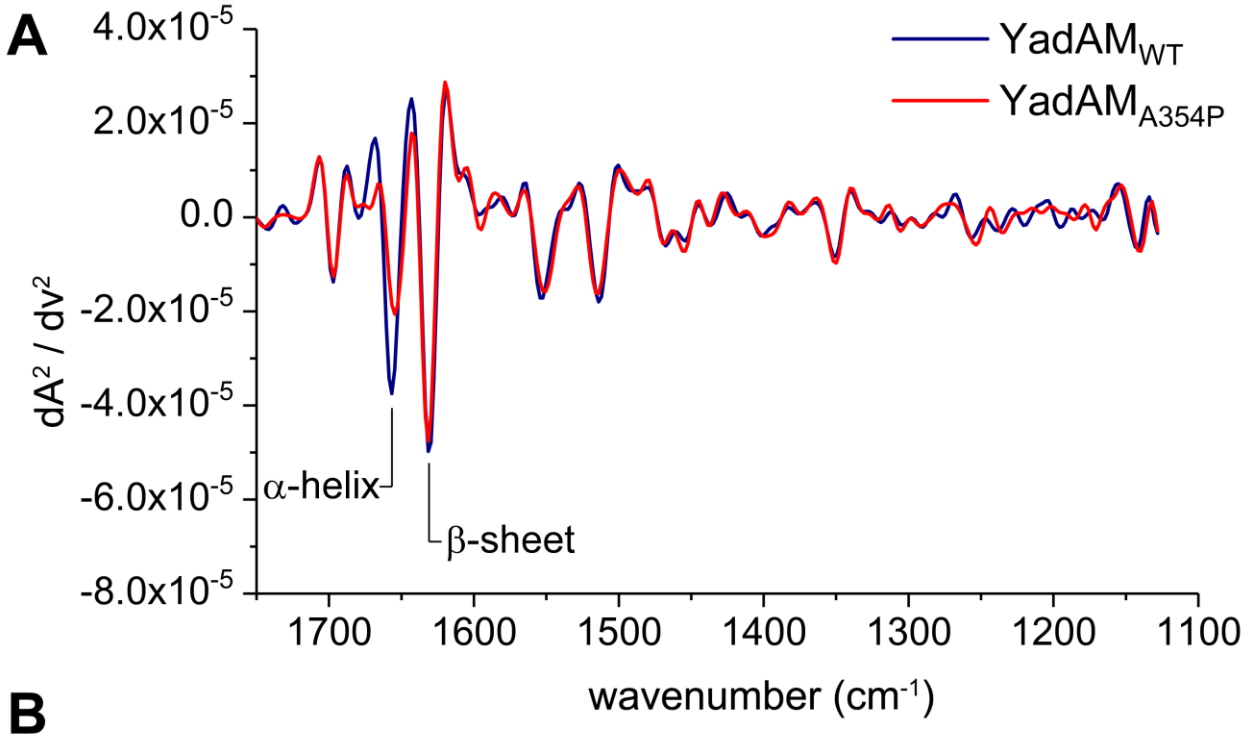

B

	α-helix (%)	β-sheet (%)	Protein concentration (mg/mL)
YadAM$_{WT}$	38.38	32.05	3.87
YadAM$_{A354P}$	25.72	33.31	4.09

Figure 7

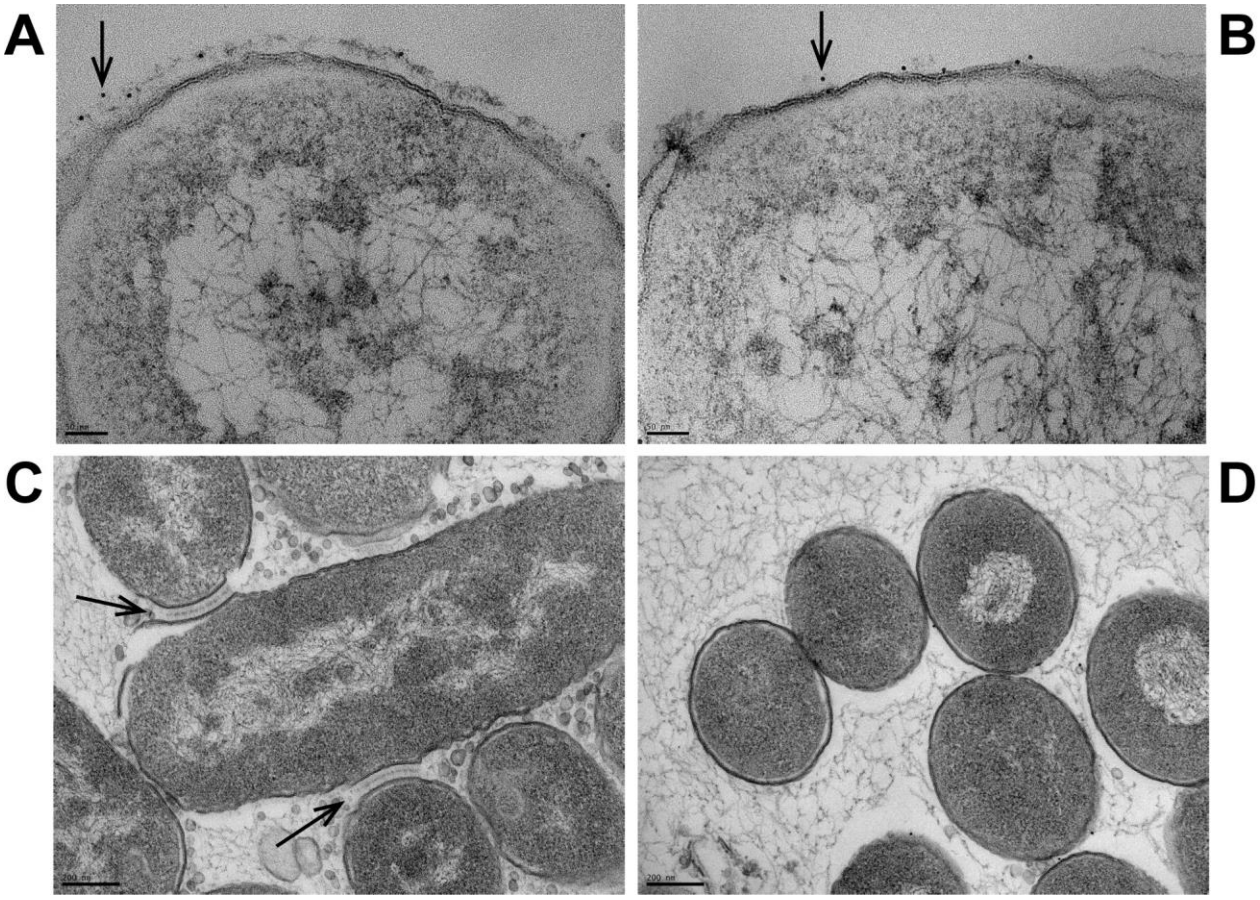

Figure 8

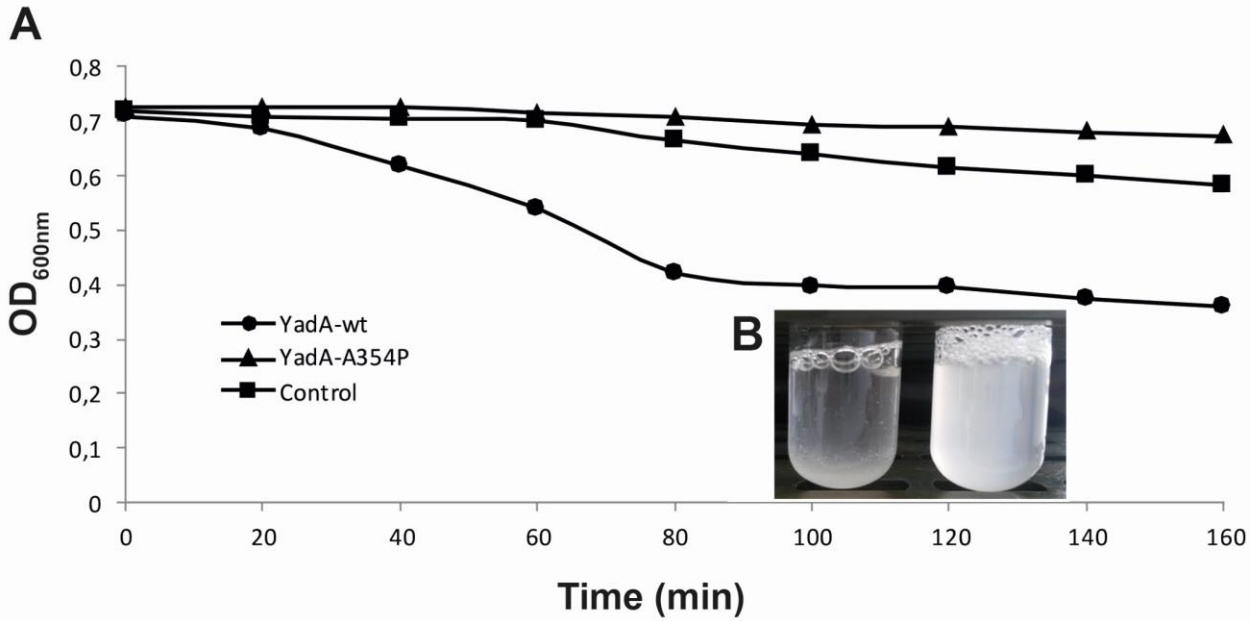
A
0,8
0,7
0,6
0,5
0,4
0,3
0,2
0,1
0
OD600nm
YadA-wt
YadA-A354P
Control
B
0
20
40
60
80
100
120
140
160
Time (min)

Figure 9

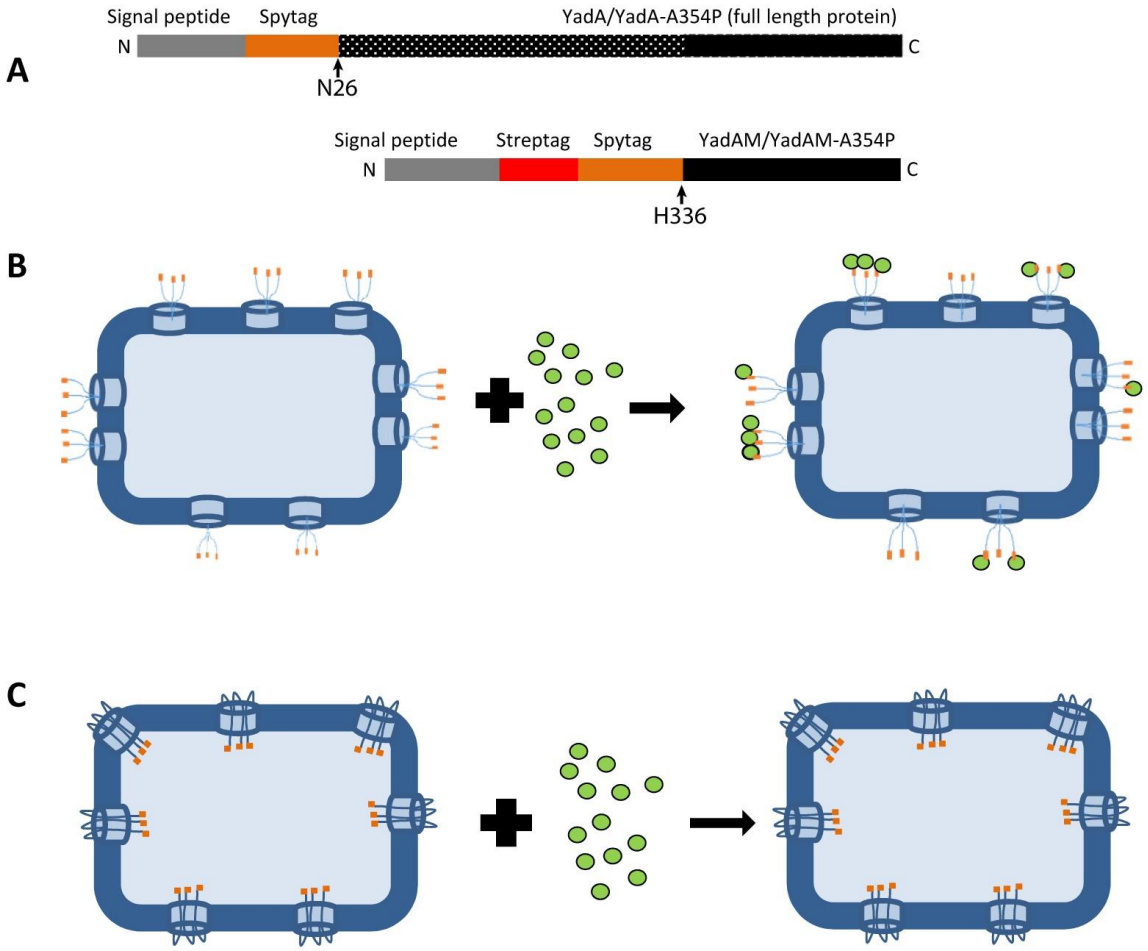
A
Signal peptide
Spytag
YadA/YadA-A354P (full length protein)
N
C
N26
Signal peptide
Streptag
Spytag
YadAM/YadAM-A354P
N
C
H336
B
C

Figure 10

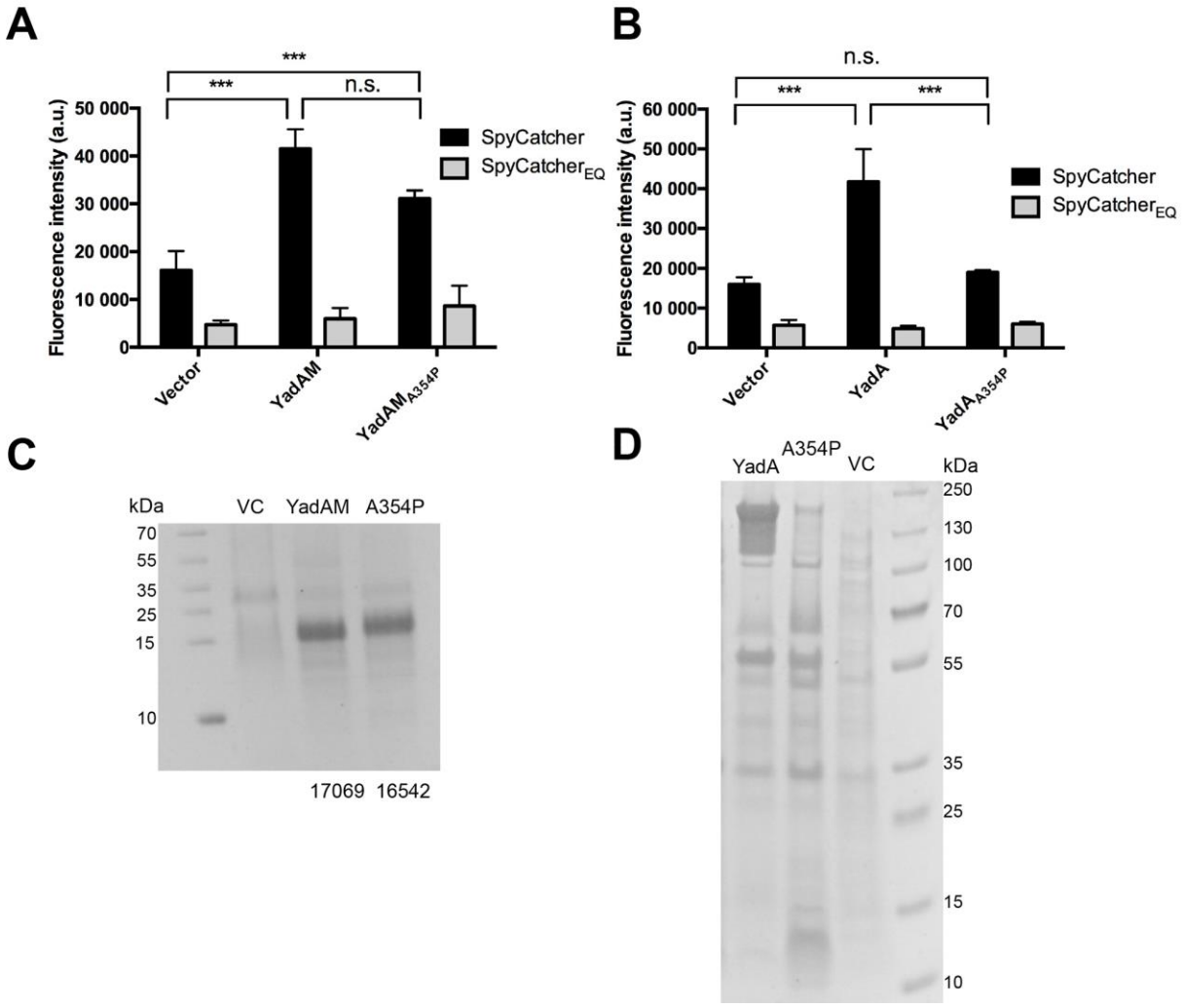
A
***
***
n.s.
Fluorescence intensity (a.u.)
50 000
40 000
30 000
20 000
10 000
0
SpyCatcher
SpyCatcher$_{EQ}$
Vector
YadAM
YadAM$_{A354P}$
B
n.s.
***
***
Fluorescence intensity (a.u.)
60 000
50 000
40 000
30 000
20 000
10 000
0
SpyCatcher
SpyCatcher$_{EQ}$
Vector
YadA
YadA$_{A354P}$
C
kDa
VC
YadAM
A354P
70
55
35
25
15
10
17069
16542
D
YadA
A354P
VC
kDa
250
130
100
70
55
35
25
15
10

Figure 11

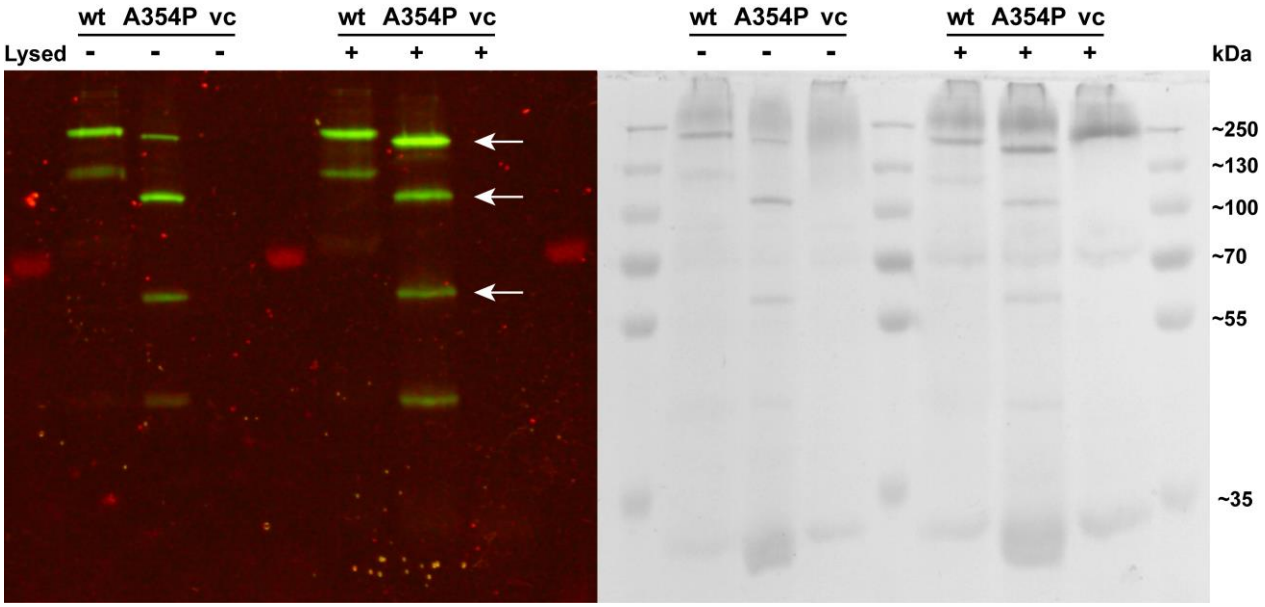

Figure 12